



MAGNETIC DIPOLE-QUADRUPOLE INTERACTION  
FIELD OF NEUTRON STAR

By  
Gemechu Muleta Kumssa

A THESIS SUBMITTED TO  
THE DEPARTMENT OF PHYSICS

PRESENTED IN PARTIAL FULFILLMENT OF THE REQUIREMENTS  
FOR THE DEGREE OF MASTER OF SCIENCE IN PHYSICS

ADDIS ABABA UNIVERSITY  
ADDIS ABABA, ETHIOPIA  
JUNE 2013

ADDIS ABABA UNIVERSITY  
SCHOOL OF GRADUATE STUDIES

This is to certify that the thesis prepared by **Gemechu Muleta Kumssa** , entitled “ **Magnetic Dipole-Quadrupole Interaction Field of Neutron Star**” and submitted in partial fulfillment of the requirements for the degree of **Master of Science** in physics.complies with the regulations of the University and meets the accepted standards with respect to originality.

Signed by the Examining Committee:

Examiner: Prf A.V.Gholap Signature: \_\_\_\_\_ Date: \_\_\_\_\_

Examiner: Prof Singh.P Signature: \_\_\_\_\_ Date: \_\_\_\_\_

Advisor: Dr.Legesse.W.K Signature: \_\_\_\_\_ Date: \_\_\_\_\_

# Abstract

Pulsars are fast spinning ( $\sim 10^4$  Hz) and highly magnetized ( $10^{13-14}G$ ) neutron stars(NSs), compact objects ( $R \sim 10$  km,  $\rho \sim 10^{13-14}g/cm^3$ ) resulting from supernova explosions that normally occur at the ends of the lives of massive stars. Measurements of electromagnetic emission related to curvature radiation from known pulsars such as Crab or Vela pulsar strongly indicate that the magnetic field structure near the surface of these objects significantly differ from the customarily expected pure star centered dipole structure. Scientists now believe that possible non-dipolar components in the magnetic field structure will resolve this long time issue. The structure of magnetic field lines also defines the type and geometry of accretion discs around neutron star in binaries. In this thesis we have determined the geometry of the combined dipole and quadrupole magnetic field lines. In idealized situations the field lines near these compact objects are closed; but they may be open at large distances due to interactions with magnetic fields or stress energy from other sources such as the accretion discs, for example. The method we used is simulating field line with matlab. The result shows the field lines are open at a given distance from the surface of the star (at  $r_{max}$ ) and it has only one solution of  $r(\theta)$  for a specific angle in one quadrant. There are three neutral lines for  $r(\theta)$  and the field line is more bulged than the pure dipole and quadrupole.

# Acknowledgements

First of all, I would like to thank the almighty God for letting me to accomplish this study. Secondly, I would like to express my heart felt gratitude to my advisor Dr. Legesse Wetro, for his invaluable advices, continuous support and friendly approach through out this research. My strongest thanks goes to my Father and Mother for they are the hero of my success .I am also thankful to my Colleague Abera Gure for his brotherly support.

Addis Ababa University  
June,2013

Gemechu Muleta Kumssa

b

*Dedicated To My Father and Mother*

# Table of Contents

<b>Abstract</b>	<b>iii</b>
<b>Acknowledgements</b>	<b>iv</b>
<b>Table of Contents</b>	<b>vi</b>
<b>List of Figures</b>	<b>viii</b>
<b>Introduction</b>	<b>1</b>
<b>1 Neutron stars</b>	<b>3</b>
1.1 The Birth of Neutron Stars . . . . .	3
1.2 Discovery of Neutron Stars . . . . .	4
1.3 Classification of Neutron Stars . . . . .	5
1.3.1 Pulsars . . . . .	5
1.3.2 Magnetars . . . . .	6
1.4 Structure of a Neutron Star . . . . .	7
1.5 Ultra-Strong magnetic fields . . . . .	8
1.5.1 Nova,Supernova and X-ray bursts . . . . .	9
1.5.2 Core-Collapse Supernovae . . . . .	10
1.5.3 Explosion Mechanisms . . . . .	12
1.6 Magnetic Field Generation of Neutron Star . . . . .	14
1.6.1 Conservation of angular momentum . . . . .	15
<b>2 Magnetic Multipole</b>	<b>17</b>
2.1 Vector potential expansion . . . . .	18
2.2 Magnetic Multipolar fields of neutron star . . . . .	23
2.2.1 Magnetic dipole filed of neutron star . . . . .	24
2.2.2 Magnetic Quadrupolar field of neutron star . . . . .	25
2.2.3 Magnetic Octupolar field . . . . .	28
2.2.4 Magnetic Dipole-Quadrupole field interaction . . . . .	28
<b>3 Magnetic multipole field line equations of neutron star</b>	<b>30</b>
3.1 Magnetic Dipole field line . . . . .	30
3.2 Magnetic Quadrupole field line . . . . .	32
3.3 Equadtion of magnetic dipole-quadrupole interaction field line and its geometry . . . . .	34

<b>4 Result and Discusion</b>	<b>37</b>
4.1 Result . . . . .	37
4.2 Discusion . . . . .	38
<b>Conclusion</b>	<b>39</b>
<b>Appendix</b>	<b>40</b>
<b>References</b>	<b>42</b>

# List of Figures

1.1	pulsating neutron star . . . . .	6
1.2	Model of a neutron star internal structure . . . . .	7
1.3	During the shock reheating phase, the stellar core is composed of a central radiating proto-neutron star whose surface is defined by the neutrinospheres (represented here by a single sphere) and a region above the neutrinosphere consisting of a net cooling region and a net heating region below the stalled shock, separated by the gain radius at which heating and cooling balance. Heating and cooling are mediated by electron neutrino and antineutrino absorption and emission . . . . .	11
1.4	The Supernova explosion. . . . .	13
1.5	A rotating neutron star. . . . .	16
2.1	Graphical comparison of neutron star magnetic multipole fields and the dipole-quadrupole interaction field vs $r$ (distance from the center of the star). As seen from the graph octupolar field is fast decaying field as $r$ increases whereas the dipole-quadrupole interaction field is strongest at the surface of the star. . . . .	29
3.1	Pure magnetic dipole field line geometry for $K_d > 1$ . . . . .	32
3.2	Pure quadrupole field line geometry for the solution we derived above. . . . .	33
3.3	Dipole-Quadrupole interaction field line geometry for specific $k$ . . . . .	35
3.4	Dipole-Quadrupole interaction field lines geometry for $k = n$ , as number of $k$ increases large space needed to see full line here. . . . .	36
4.1	Graphical representation of field lines for neutron star magnetic dipole-quadrupole interaction, where $\theta$ is in radians. . . . .	37
4.2	Graph of magnetic pure dipole and quadrupole field lines and their interaction. . . . .	38

# Introduction

Our universe consists of elementary particles (electron, proton, neutron, positron, neutrino, and photon, etc.) and massive bodies (stars, galaxies, and so on). Stars are formed in molecular clouds in the interstellar medium, which consist mostly of molecular hydrogen (primordial elements made a few minutes after the beginning of the universe) and dust. The dust originates from the cool surfaces of supergiants, massive stars in a late stage of stellar evolution. This dust is an irregularly shaped grains of carbon or silicate measuring a fraction of a micron across which is found between the stars [1]. The night sky contains myriads of stars including those in the Milky Way, which is a side view of our Galaxy looking along the plane of the disc. Our Galaxy includes about  $10^{11}$  stars. Beyond our galaxy are billions of other Galaxies. The nearest star is Proxima Centauri it is about 4 light years away and the nearest large Galaxy is Andromeda is about 2 million light year away. Our Galactic disc has a diameter of about 100,000 light years [2].

Basic factors in the formation of stellar objects are gravity, dust, gas pressure, rotation, magnetic fields, winds and radiation from nearby young stars and radiative shock waves. Building a comprehensive physical picture of stellar structure and evolution is one of the greatest triumphs of 20th century Astrophysics. However, many important aspects of the life cycle of stars are still not completely understood [3]. They include: the origin and evolution of stellar magnetic fields, including the large-scale fields, the sun-spot cycle, the evolution of the stellar rotation, the origin and character of differential rotation, high-energy coronal activity, mass loss in massive stars and various aspects of binary evolution [4].

Even more critical questions remain open regarding the end of the life of stars and their afterlife as compact objects [5,6]. These include the mechanisms of core-collapse supernovae (SNe) and gamma-ray bursts (GRBs), the origin of magnetars, the workings of radio-pulsars and pulsar-wind nebulae, some aspects of accretion disks and jets in binary systems [7]. All these questions are at the forefront of modern Astrophysics. Importantly, many of them unavoidably involve magnetic fields interacting with the plasma. Therefore, they belong to the realm of Plasma Astrophysics. A common theme in plasma astrophysics is the life cycle of magnetic fields: How are they produced (dynamo)? How do they interact with the plasma (magnetic braking, magnetocentrifugal wind acceleration, MHD instabilities such as MRI)? And how are they destroyed (reconnection)[8]?

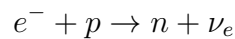
In this thesis we will consider the complex magnetic fields of a compact star called neutron star. Observations and theory suggest that complex multipolar magnetic fields prevail near the surface of neutron stars and play an important role in the physics of rotation powered pulsars [4]. Objectives of the thesis are: deriving field line equation for magnetic dipole-quadrupole combination of neutron star modeling (simulating) the geometry of this interaction field lines in 2-dimension, finding neutral points for this line.

# Chapter 1

## Neutron stars

### 1.1 The Birth of Neutron Stars

NSs are one of the possible ends for stars. They result from massive stars which have mass greater than 4 to 8 times that of our Sun. After these stars have finished burning their nuclear fuel, they undergo a supernova explosion [11,4]. This explosion blows off the outer layers of a star into a beautiful supernova remnant. The central region of the star collapses under gravity. It collapses so much that protons and electrons combine to form neutrons according to the reaction



A NS is supported by the pressure of cold degenerate neutrons, almost all electrons and protons having been converted into neutrons through reaction the neutrinos escaping from the star. At higher densities the most important correction is due to the inverse  $\beta$ -decay. The condition for the inverse  $\beta$ -decay ( $e^{-} + p \rightarrow n + \nu_e$ ) is that the kinetic energy of the electrons be larger than or equal to  $1.36\text{MeV}$ . The  $\beta$ -decay of a neutron ( $n \rightarrow e^{-} + p + \nu_e$ ) is blocked when the density is so large that all the electron levels in the Fermi sea are filled up to the energy of the emitted electron. Hence the name "Neutron Star" [12]. A NS is about 20 km in diameter and has the mass of about 1.4 solar mass. This means that a NS is so dense that on Earth, one teaspoonful would weigh a billion tons! Because of its small size and high density, a NS possesses a surface gravitational field about  $2 \times 10^{11}$  times that of Earth [11,13].

NSs can also have magnetic fields a million times stronger than the strongest magnetic fields produced on Earth. NSs may appear in supernova remnants, as isolated objects, or in binary systems.

When a NS is in a binary system, astronomers are able to measure its mass [11,14]. If a neutron star is rotating rapidly, as most young NSs are, the strong magnetic fields combined with rapid rotation create an awesome generator that can produce electric potential differences of quadrillions of volts [15,13]. Such voltages, which are 30 million times greater than those of lightning bolts [16], create deadly blizzards of high energy particles [17]. The neutron star which we currently rank as "nearest to Earth" is a radio pulsar called J0108-1431. It is within about 100 parsecs away from our planet.

## 1.2 Discovery of Neutron Stars

On 28 of November 1967 the Mullard Radio Astronomy observatory array observed a train of pulses of varying amplitudes but quite regular spacing near  $19^h 19^m$  right ascension and 21 degrees (+) of northern declination [11,18]. It was not at first realized what exactly had been observed (given especially that an automobile ignition could produce such a regular pattern of interference), but Jocelyn Bell, a research student, eventually found the observation to be genuine and was assigned the task of identification. Ultimately a Nobel Prize went to the discovery director [11,13], Anthony Hewish. The year 1979 was a remarkable one for the study of soft gamma repeaters (SGRs), although nobody realized it at the time [11,15,18]. The first SGR burst ever detected, from a source in constellation Sagittarius [19,14], occurred on January 7, 1979.

Then a truly powerful SGR outburst indeed, by far the most intense blast of gamma-rays that had ever been detected from outside our solar system (until another SGR out burst broke the record in 1998) came just two months later, on

March 5, 1979. This tremendous flare eventually allowed the SGR mystery to be unraveled. Only nine days after that a third SGR became active in a new part of the Galaxy, giving three bursts in a three day period. So during the first three months of 1979, three of the five known SGRs were discovered [12, 17, 8].

## 1.3 Classification of Neutron Stars

According to their magnetic fields, neutron stars are classified into two, namely, pulsars and magnetars with typical polar surface magnetic fields of  $10^{12} - 10^{13}$  G and  $10^{14} - 10^{15}$  G, respectively [20, 11]. Magnetars are subdivided into soft gamma repeaters (SGRs) and anomalous X-ray pulsars (AXPs) [20, 21, 11]

### 1.3.1 Pulsars

Pulsars (pulsating radio stars) are the class of cosmic objects that populate the plane of our galaxy in the Milky Way and rapidly rotate by emitting extremely regular pulses of radio waves, with several such objects known to emit pulses of visible light, X-rays and gamma-rays as well [20, 22]. Ordinary radio pulsars are NSs with magnetic fields  $\sim 10^{12}$  Gauss and spin periods between 16 milliseconds and 8.5 seconds [20]. They are also radio "loud" for approximately 10 million years being powered by the loss of the rotational energy that the star is born with [9, 23]

A radio pulsar is a NS in which large-scale dynamo has essentially failed to operate, because it is not born fast enough (compared to the magnetar) as a result pulsar magnetic field is essentially stable [9, 19]; its main role is to passively facilitate the loss of rotational energy. NSs have been observed to "pulse" radio and X-ray emissions believed to be caused by particle acceleration near the magnetic poles, which need not be aligned with the rotation axis of the star [13]. Through mechanisms not yet entirely understood, these particles produce coherent beams of radio emission. External viewers see these beams as pulses of radiation whenever the magnetic pole sweeps past the line of sight. The pulses come at the same rate

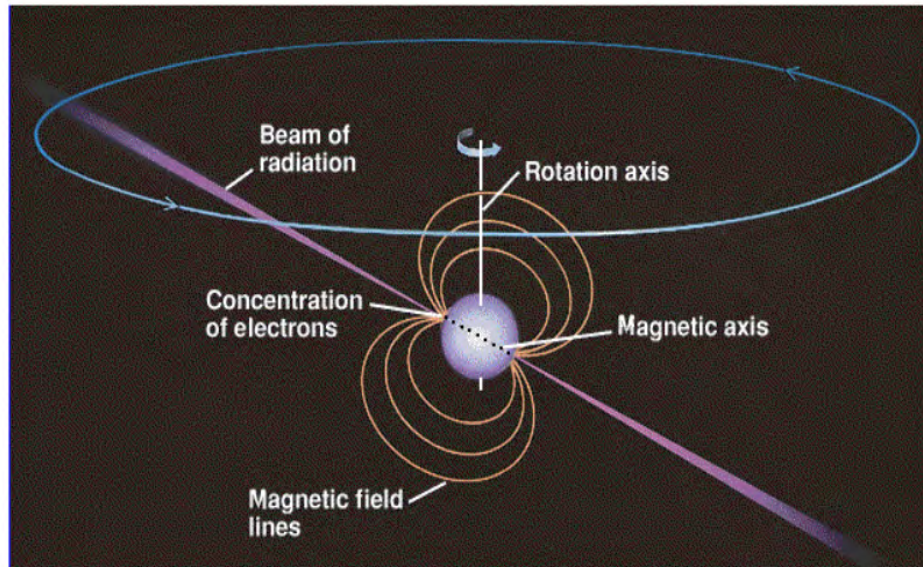


Figure 1.1: pulsating neutron star

as the rotation of the neutron star and thus, appear periodic. Neutron stars which emit such pulses are called pulsars.

### 1.3.2 Magnetars

Magnetars (AXPs and SGRs) are kinds of very compact NSs a city-sized ball of neutrons created from star core when a dying star ( $M \geq 25M_{\odot}$ ) explodes as a supernova at the end of its life. Young magnetars have magnetic fields that range from approximately  $10^{14} - 10^{15}$  G and they are born spinning faster than pulsars[11,13]. In magnetar, the combined effects of rotation and convection can build up the magnetars magnetic field through dynamo process. But the rotational energy quickly decreases and the magnetic field itself provides an energy source for emission. As a result of this a magnetars magnetic energy is dissipated during the first 10,000 years[11,21].

## 1.4 Structure of a Neutron Star

One of the important aspects in the study of neutron stars is the equation of state, i.e., the functional dependence of the pressure  $P$  on the density  $\rho$  [4,9]. In the interior of neutron stars the nuclear matter is found at densities above the neutron drip  $\rho_d \approx 4 \times 10^{11} g/cm^3$ . The properties of cold dense matter and the associated equation of state are reasonably well understood at densities up to  $\rho_n \approx 3 \times 10^{14} g/cm^3$ . In the high-density range above  $\rho_n$  the physical properties of matter are still uncertain [18]. Typical neutron stars have masses in the range

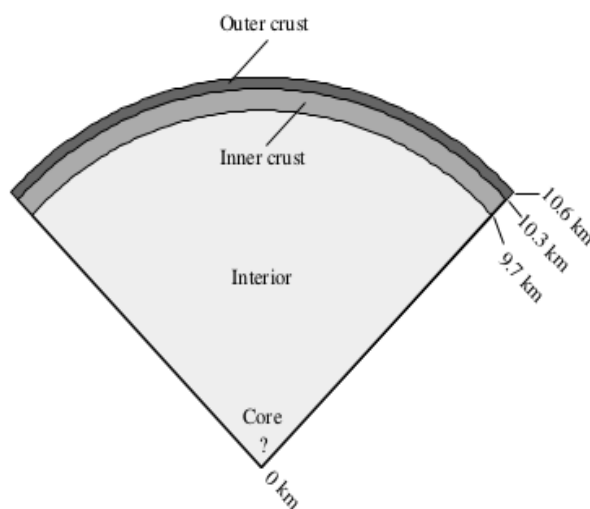


Figure 1.2: Model of a neutron star internal structure

( $M \sim 1.4M_{\odot}$ ) and radii of the order of  $R \sim 10 km$ . The different regions of the star are described as follows.

- The surface for ( $\rho < 10^6 g/cm^3$ ) is a region in which the temperatures and magnetic fields significantly affect the equation of state.
- The outer crust for ( $10^6 g/cm^3 \leq \rho \leq 4 \times 10^{11} g/cm^3$ ) is a solid region in which a Coulomb lattice of heavy Iron nuclei coexists in  $\beta$ -equilibrium with a relativistic degenerate electron gas.
- The inner crust for ( $4 \times 10^{11} g/cm^3 < \rho < 2 \times 10^{14} g/cm^3$ ) consists of a lattice of neutron-rich nuclei together with a superfluid neutron gas and electron gas.

- The neutron liquid ( $2 \times 10^{14} g/cm^3 < \rho < 8 \times 10^{14} g/cm^3$ ) contains mainly superfluid neutrons with a smaller concentration of superfluid protons and normal electrons.
- The core region for ( $\rho > 8 \times 10^{14} g/cm^3$ ) may or may not exist in some neutron stars, and will depend on whether or not kaon condensation or pion condensation occurs [11], or whether there is a transition to neutron solid or quark matter or some other phase of hyperons physically distinct from a neutron liquid in the core. The core could, for instance, contain geometrically mixed phases of nuclear and quark matter [8], where the geometries may be idealized as drops, rods and slabs. There could be an inner sphere of pure quark matter surrounded by a crystalline region of mixed hadronic and quark matter.

The mixed phase region then consists of various geometrical objects of the rare phase immersed in the dominant one, from hadronic drops immersed in quark matter to quark drops immersed in hadronic matter [15]. The particle composition of these regions then should be quarks, nucleons, hyperons and leptons [18]. A liquid of neutron star matter containing nucleons and leptons would surround the mixed phase, and a crust of heavy ions should form the stellar surface.

## 1.5 Ultra-Strong magnetic fields

Many fascinating physical effects occur in magnetic fields with strength exceeding the Quantum critical field of  $B_Q = 4.4 \times 10^{13}$  G. (This field-strength is given by a combination of fundamental constants:  $B_Q = \frac{m_e^2 c^3}{e \hbar}$ , where  $m_e$  is the mass of an electron,  $c$  is the speed of light,  $\hbar = \frac{h}{2\pi}$ , and  $e$  is the charge of an electron) [11,15]. This field strength determines the luminosity, the life time, and even the nature [20] of the energy loss from isolated neutron stars. In fields stronger than  $B_Q$ , electrons gyrate nearly the speed of light around magnetic field lines, even in their lowest quantum energy states. Consequently, the ultra-magnetized vacuum which [25,26], according to quantum mechanics, seethes with virtual electron-positron pairs and other particles becomes birefringent like a calcite crystal, capable of

destroying and magnifying images(”magnetic lensing”)[27,13,28]. X-ray photons travelling through such strong fields readily split into two, or merge together; and many other novel physical effects come into play because  $B_Q$  lies between the field strengths observed in magnetars and in ordinary radio pulsars [24],this new physics is important in making the theory of magnetars[29].Although magnetar fields are stronger by most measures, they are weak compared to the strongest possible field that could theoretically exist in nature, which is  $10^{49} - 10^{53}$  Gauss [20,21].A field stronger than this would literally break down the vacuum and decay, via the quantum mechanical process of magnetic monopole creation.However,there is no known way that such strong fields could be generated.Magnetars are the most strongly-magnetized objects yet known in the universe.

### 1.5.1 Nova,Supernova and X-ray bursts

Supernovae,novae and X-ray bursts are similar in that they both involve the sudden release of large amounts of energy. In the case of novae and X-ray bursters,the energy comes from runaway fusion on the surface of a compact object in a binary. In contrast,the source of energy for a supernova is the core collapse of a massive star [11,9]. In a nova, the fusion occurs on the surface of a white dwarf, while it occurs on the surface of a neutron star in X-ray bursters[2]. In a nova, the fusion is hydrogen fusion, but in an X-ray burster, the hydrogen has fused into helium on the neutron star surface, so the burst comes from helium fusion. A supernova also has a remnant distinct from its progenitor in contrast to a nova or X-ray burst which leaves the progenitor little different.This is also the reason that supernovae are one-time events in contrast to the reoccurring novae and X-ray bursters[2].

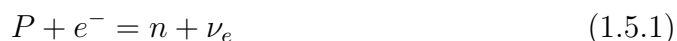
In general a supernova explosion is the end of the life of a massive stars.The energy released during this possibly, would take 10 billion years for our Sun to deliver the same energy output. During a NS formation most of the energy released is in the form of scarcely observable neutrinos. The energy flash it self comes either from

the thermal instability developed in the degenerate core, or from gravitational and partly nuclear energy release during the collapse [19,9].

The magnetic field and rotation play an important role in converting gravitational energy into the energy of an observable flash. A small number of stars (the most massive once) end their lives in gravitational collapse and black hole formation. The collapse in this case may be silent and not lead to supernova explosion [12]. Supernovae (SNe) eject over 90 percent of the dying star mass into interstellar space with a kinetic energy of the order of  $10^{51}$  erg [7,18]. The ejecta contain heavy elements that are important for the chemical evolution of galaxies, stars, planets, and life.

### 1.5.2 Core-Collapse Supernovae

During the last stage of a stellar evolution, nuclear burning takes place until an iron core is formed via H, He, C, O, Ne, and Si burnings [9,4]. Since iron is the most stable element, further nuclear burning does not occur, and after a while the iron core begins to contract under the gravity of the star [9]. The contraction increases the density and temperature, and when the density reaches up to the onset of electron capture, or when the temperature reaches up to the photodisintegration of the nuclei, the pressure decreases and gravitational collapse is set about [9]. The collapse continues until the central density reaches the nuclear density, in which the pressure at the center of the core becomes sufficiently large to prevail the local gravity with the help of the nuclear force. Under such extreme conditions electron degeneracy cannot support the stellar core, and the free electrons are forced to join with protons to form neutrons (inverse beta decay):



The neutrinos, which escape directly from the core result in further energy loss and even faster collapse. The core collapses so rapidly that it effectively collapses out from under the stellar envelope.

Collapse is halted only if nuclear matter under compression can stiffen sufficiently. Otherwise black holes result [19,9]. The collapsing core divides into two regions: an inner core, homologously collapsing, subsonic core (infall velocities proportional to radius) and an outer supersonic shell. Then Bounce occurs and a shock wave is generated at the boundary of the inner and the outer core. If the shock wave propagates through the core and the stellar envelope, blowing off matter, this results in a supernova explosion. On the other hand the inner core remains as a proto-NS which soon evolves into a NS after a cooling timescale of  $\sim 5 - 10s$  [23]. The neutrinos generated are out gradually after the bounce with a timescale of  $\sim 500ms$ ,

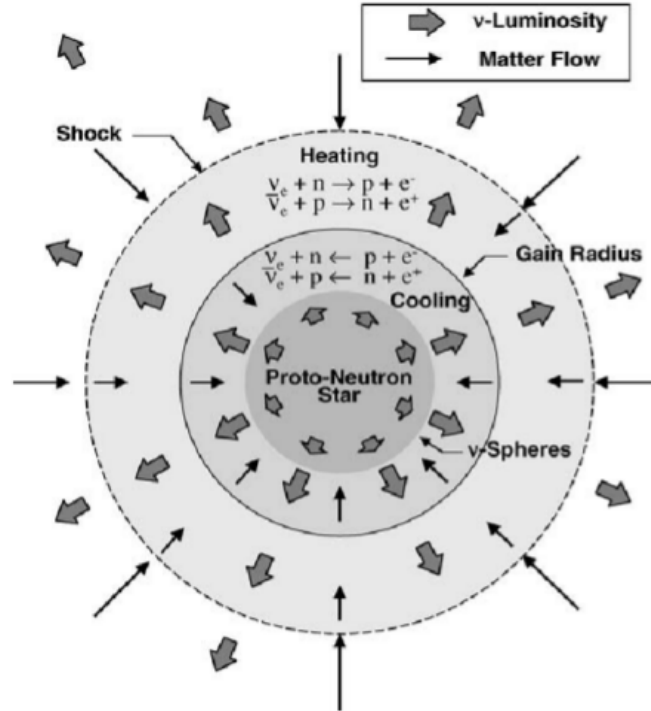


Figure 1.3: During the shock reheating phase, the stellar core is composed of a central radiating proto-neutron star whose surface is defined by the neutrinospheres (represented here by a single sphere) and a region above the neutrinosphere consisting of a net cooling region and a net heating region below the stalled shock, separated by the gain radius at which heating and cooling balance. Heating and cooling are mediated by electron neutrino and antineutrino absorption and emission

and heat up matter behind the stalled shock wave via weak interaction. If the heat

from the neutrinos is ample, the stagnated shock wave would revive and propagate through the core again. This is, however, denied by the recent spherically symmetric simulations which employ a realistic equation of state (EOS) and deal with sophisticated microphysics such as neutrino transport and/or electron capture, in which successful explosions have not been found [12,2] the core resulting from the evolution of a star in the higher mass range collapses because it surpasses the critical Chandrasekhar limit. The core mass approaches  $M_c \approx 1.44M_\odot$  the core radius  $R_c = 0.01R_\odot$  where  $(R_\odot = 6.9599 \times 10^{10}cm) \sim 7 \times 10^{10}cm$  is a stellar radius. The interior matter density increases [4], speed up by the ongoing electron capture. When a stellar interior neutronizes, reducing the number of particles by a factor 2, but more importantly, eliminating the electric charges, the implosion generates a very densely packed core of neutrons of typically  $R_N = 10km$ . The collapse time (the free-fall time) is about 1s. At the same time, shell material is pulled in and falls onto the core [9,4]. During this time gravitational energy is released to the amount of

$$E_G = \frac{GM_c^2}{R_N} \approx 3 \times 10^{53}erg \quad (1.5.2)$$

Note that the total observed energy of such a SN out-burst (kinetic energy, electromagnetic energy plus energy in neutrinos) is roughly  $10^{53}$  erg.

### 1.5.3 Explosion Mechanisms

When the core of progenitor star has collapsed down to a size of about 10 km, neutron degeneracy sets in causing the core to stiffen and the infalling material from the envelope to rebound in a shock-wave outward from the core [1,8]. It was this bounce shock that originally looked like a good candidate for the mechanism that produces the supernova explosion. The shock never reaches the outer layers of the star with enough energy to explode them, because of severe energy losses on the way. Energy losses to the shock are from two sources, dissociation of heavy nuclei into lighter components and production and escape of some neutrinos; both follow from the heat and entropy generated by the energetic shock [9].

The major way in which this loss occurs is through photodisintegration (a process that cools the shock on a hydrodynamical time-scale, immediately following core bounce, is the passage through it of neutrinos emitted from regions behind it, as the shock moves outward). Neutrinos are the key to supernova explosion: these are emitted copiously from the hot, collapsed core (and thereby cool the core, as we mentioned above, carrying away the gravitational binding energy released in the formation of the neutron star), and these neutrinos would stream through, deposit some fraction of their energy and momentum in the outer stellar layers ahead of the shock, and explode them away [4,5].

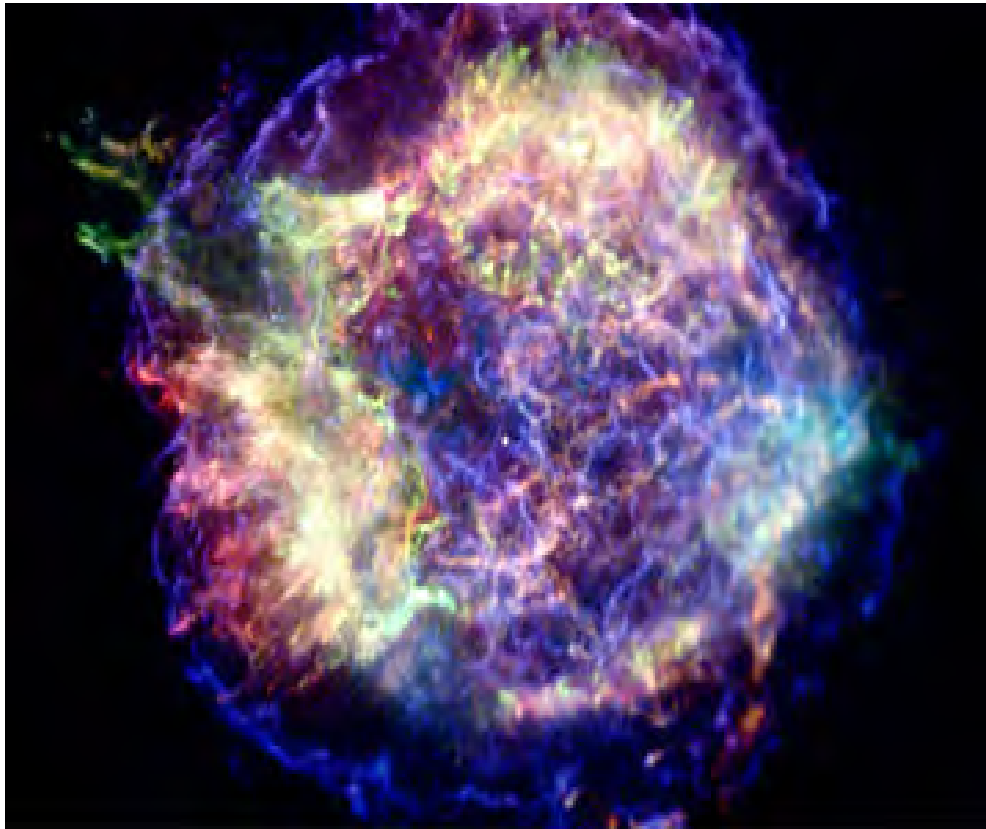


Figure 1.4: The Supernova explosion.

## 1.6 Magnetic Field Generation of Neutron Star

The origin of strong magnetic fields in neutron stars is still a matter of controversy [7,30]. The present understandings are:

1. The standard theory simply related to the magnetic fields of the progenitor main sequence stars frozen during collapse or flux conservation (Woltjer,1964). This model does not deliver the mechanism for the generation of magnetic multipoles. It can not generate field strength of magnitude about  $10^{16}$  G often observed in GRB activities such very strong magnetic fields are required force for supernova bounce since the energy of the shock blast normally gets dissipated half way through the infalling iron core.

2. Naturally if they are generated through a dynamo mechanism driven by turbulent motions. This is opposed by several theorems such as Cowley's theorem.

3. The generation of neutron star magnetic fields by thermomagnetic effects. This is a model which requires along time ( $\sim 10^3$  years) to generate a surface magnetic field of ( $\sim 10^{12}$  G) provided that there is an original field of ( $\sim 10^8$  G) which could come from flux conservation. This is why too slow and too weak to describe such violent processes as GRBs etc.,.

4. By the spinning of separated charges.

This model is able to generate field strengths up to  $\sim 10^{18}$  G enough to meet all requirements of current experimental findings. Most importantly it very clearly indicates that NS surface fields have infinite multipoles a fact we use in this thesis.

### 1.6.1 Conservation of angular momentum

A rotating object has angular momentum  $L$  given by

$$L = I\Omega \quad (1.6.1)$$

Where  $I$  is the moment of inertia  $\Omega$  is the angular velocity it is the angle in radians through which an object rotates per unit time. If the rotation period is  $T$  then:  $\Omega = \frac{2\pi}{T}$ . The moment of inertia of a uniform sphere of mass  $M$  and radius  $R$  is

$$I = \frac{2}{5}MR^2 \quad (1.6.2)$$

$I = \frac{2}{5}MR^2 \approx 10^{45} \text{ gcm}^2$  for a neutron star. Therefore, before it collapses to a neutron star, the core of a progenitor star has an angular momentum of

$$L = \frac{2}{5}MR_o^2\Omega_o^2 = \frac{2}{5}MR_o^2\frac{2\pi}{T_o} \quad (1.6.3)$$

Angular momentum and core mass is conserved during the collapse, so after the neutron star forms it will have the same  $L$  (angular momentum)

$$L = \frac{2}{5}MR_o^2\frac{2\pi}{T_o} = \frac{2}{5}MR_{Ns}^2\frac{2\pi}{T_{Ns}} \quad (1.6.4)$$

so the rotation period of the neutron star is found to be

$$\tau_{Ns} = \left(\frac{R_{Ns}}{R_o}\right)^2 T_o \quad (1.6.5)$$

Suppose the core of an atypical dying star has a radius of  $7 \times 10^5 \text{ Km}$  and rotates once every 30 days i.e.  $\sim 2.6 \times 10^6 \text{ s}$ . After collapsing to a neutron star of radius  $10 \text{ Km}$  it will have a rotation period of

$$T_{Ns} = \left(\frac{10 \text{ Km}}{700,000 \text{ Km}}\right)^2 2.6 \times 10^6 \text{ s} = 0.000528 \text{ s} \simeq 0.53 \text{ ms} \quad (1.6.6)$$

So we have an object of about the mass of the sun rotating  $\simeq 1,884$  times every second, i.e.  $\frac{2.6 \times 10^6 \text{ s}}{0.0005 \text{ s}} = 4.9 \times 10^9$  this implies  $\frac{4.9 \times 10^9}{2.6 \times 10^6 \text{ s}} = 1,884 \text{ s}^{-1}$ . In other words, the sun rotates  $4.9 \times 10^9$  times more slowly than the neutron star. The neutron star is born with a spin period of about 0.5 ms. This is very, very fast, and only a neutron star or a black hole could sustain such rapid rotation without flying apart.

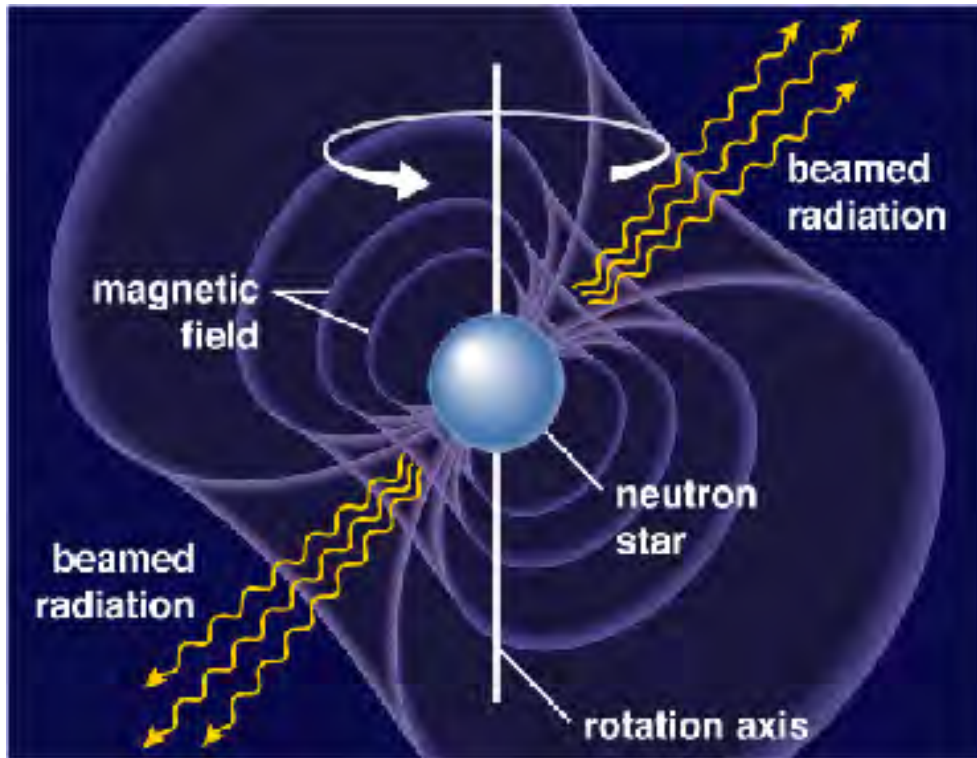


Figure 1.5: A rotating neutron star.

Strong jets of matter are emitted at the magnetic poles. If the rotation axis is not the same as the magnetic axis, the two beams will sweep out circular paths. If the Earth lies in one of those paths, we will see the star pulse. Pulsars radiate their energy away quite rapidly; the radiation weakens and stops in a few tens of millions of years [15,20], making the neutron star virtually undetectable.

## Chapter 2

# Magnetic Multipole

In this chapter we derive magnetic multipoles of an arbitrary vector potential  $\vec{A}(\vec{r})$  given in spherical coordinates. For each pole we derive the equation of the field lines. The magnetostatic Maxwell's equation can be written in general form for a current density [31,29,32]  $\vec{J}(\vec{r})$  as

$$\vec{B}(\vec{r}) = \frac{\mu_0}{4\pi} \int \vec{J}(\vec{r}') \times \frac{\vec{r} - \vec{r}'}{|\vec{r} - \vec{r}'|^3} dv' \quad (2.0.1)$$

To obtain the differential equation equivalent to this we use the relation just [29,37]  $\vec{B} = \vec{\nabla} \times \vec{A}$  this implies the divergence of B vanishes.

$$\vec{\nabla} \cdot \vec{B} = 0 \quad (2.0.2)$$

This is the first Maxwell's equations for magnetostatics and corresponds to  $\vec{\nabla} \times \vec{E} = 0$  in electrostatics by analogy with electrostatics we now calculate the curl of  $\vec{B}$ :

$$\vec{\nabla} \times \vec{B} = \frac{\mu_0}{4\pi} \vec{\nabla} \times \vec{\nabla} \times \int \frac{\vec{J}(\vec{r}')}{|\vec{r} - \vec{r}'|} dv' \quad (2.0.3)$$

With the identity

$$\vec{\nabla} \times (\vec{\nabla} \times \vec{A}) = \vec{\nabla}(\vec{\nabla} \cdot \vec{A}) - \nabla^2 \vec{A}$$

for an arbitrary vector field A, the above expression can be transformed into

$$\vec{\nabla} \times \vec{B} = \frac{\mu_0}{4\pi} \vec{\nabla} \int \vec{J}(\vec{r}') \cdot \vec{\nabla} \left[ \frac{1}{|\vec{r} - \vec{r}'|} \right] dv' - \frac{\mu_0}{4\pi} \int \vec{J}(\vec{r}') \nabla^2 \left[ \frac{1}{|\vec{r} - \vec{r}'|} \right] dv' \quad (2.0.4)$$

We use

$$\vec{\nabla} \left[ \frac{1}{|\vec{r} - \vec{r}'|} \right] = -\vec{\nabla}' \left[ \frac{1}{|\vec{r} - \vec{r}'|} \right]$$

And

$$\vec{\nabla}^2 \left[ \frac{1}{|\vec{r} - \vec{r}'|} \right] = -4\pi\delta(\vec{r} - \vec{r}')$$

equation 2.0.4 can be written as

$$\vec{\nabla} \times \vec{B} = \frac{-\mu_o}{4\pi} \vec{\nabla} \int \vec{J}(r') \cdot \vec{\nabla}' \left[ \frac{1}{|\vec{r} - \vec{r}'|} \right] dv' + \mu_o \vec{J}(\vec{r}') \quad (2.0.5)$$

Integration by parts yields

$$\vec{\nabla} \times \vec{B} = \frac{\mu_o}{4\pi} \vec{\nabla} \int \frac{\vec{\nabla} \cdot \vec{J}(\vec{r}')}{|\vec{r} - \vec{r}'|} dv' + \mu_o \vec{J}(\vec{r}') \quad (2.0.6)$$

But for steady state magnetic phenomena

$$\vec{\nabla} \cdot \vec{J} = 0$$

this leads to

$$\vec{\nabla} \times \vec{B} = \mu_o \vec{J}(\vec{r}') \quad (2.0.7)$$

This is Maxwell's second equation for magnetostatics.

## 2.1 Vector potential expansion

Let us consider a charge Q uniformly distributed over the surface of spherical neutron star of radius  $R_*$ . Assume that a neutron star is spinning with a frequency of  $\Omega$  about its diameter [31,32]. We need to calculate (drive equations) for magnetic multipole fields generated by the spinning charge at the external surface of the neutron star [33,34]. The vector potential can be written in general form as

$$\vec{A}(\vec{r}) = \int \frac{\vec{J}(r')}{|\vec{r} - \vec{r}'|} dv' \quad (2.1.1)$$

But we know that

$$\vec{J}(\vec{r}') = -|\sigma|V\delta(r' - R_*)\hat{e}_\varphi \quad (2.1.2)$$

Where

$$\sigma = \frac{|Q|}{4\pi R_*^2} \quad \text{and} \quad V = \Omega \times R_* \quad (2.1.3)$$

Therefore

$$\vec{J}(\vec{r}') = -\frac{|Q|}{4\pi R_*^2} [\Omega \times R_*] \delta(r' - R_*) \hat{e}_\varphi = -\frac{|Q|}{4\pi R_*} \Omega \sin\theta' \delta(r' - R_*) \hat{e}_\varphi$$

considering that  $\vec{J}(r') = \vec{J}(r')_{\varphi'} \hat{e}_{\varphi}$  where

$$\vec{J}(\vec{r}')_{\varphi'} = -\frac{|Q|}{4\pi R_*} \Omega \sin\theta' \delta(r' - R_*) \quad (2.1.4)$$

substituting this in to the exprsion of  $\vec{A}$  we find that

$$\vec{A}(\vec{r}) = \hat{e}_{\varphi} \int \frac{\vec{J}(\vec{r}')_{\varphi'}}{|\vec{r} - \vec{r}'|} dv' \quad (2.1.5)$$

Where  $R_*$  is radius of the star. The current density  $\vec{J}$  has only a component in the  $\varphi$  direction. The vectorial current density can be written as

$$\vec{J} = -\vec{J}_{\varphi} \sin\varphi' \hat{i} + \vec{J}_{\varphi} \cos\varphi' \hat{j} \quad (2.1.6)$$

Since the integration of equation(2.1.5) is symmetric about  $\varphi = 0$  the x component of the current does not contribute. This leaves only the y-component which is  $\vec{A}_{\varphi}$ . Now let us introduce the use of Spherical harmonic expansion. For ordinary leg-ender functions to have finite solutions in the interval  $[-1, 1]$ , the parameter  $l$  must be zero or positive integer and the integer  $m$  runs from  $l$  to  $-l$ , the solution having this properties is called an associated legender function  $P_l^m(x)$ . For positive  $m$  it is defined by:

$$P_l^m(x) = (-1)^m (1-x^2)^{m/2} \frac{d^m}{dx^m} P_l(x) \quad (2.1.7)$$

where Legendre polynomial is given by

$$P_l(x) = \frac{1}{2^l l!} \frac{d^l}{dx^l} (x^2 - 1)^l \quad (2.1.8)$$

Example: the first three Legendre polynomials are:

$$P_0(x) = 1, P_1(x) = x, P_2(x) = \frac{1}{2}(3x^2 - 1), P_3(x) = \frac{1}{2}(5x^3 - 3x) \quad (2.1.9)$$

If Rodrigues formula is used to represent  $P_l(x)$ , a definition valid for both positive and negative  $m$  is

$$P_l^m(x) = \frac{(-1)^m}{2^l l!} (1-x^2)^{m/2} \frac{d^{l+m}}{dx^{l+m}} (x^2 - 1)^l \quad (2.1.10)$$

$P_l^{-m}(x)$  and  $P_l^m(x)$  are proportional since  $m$  is integer.

$$P_l^{-m}(x) = (-1)^m \frac{(l-m)!}{(l+m)!} P_l^m(x) \quad (2.1.11)$$

The first few legender functions are:

$$\begin{aligned}
P_1^0(x) &= x, & P_1^1(x) &= (1-x^2)^{\frac{1}{2}} \\
P_2^0(x) &= \frac{1}{2}(3x^2-1), & P_2^1(x) &= 3x(1-x^2)^{\frac{1}{2}} \\
P_2^2(x) &= 3(1-x^2), & P_3^1(x) &= \frac{3}{2}(5x^2-1)(1-x^2)^{\frac{1}{2}}
\end{aligned} \tag{2.1.12}$$

For fixed  $m$  the functions  $P_l(x)$  form an orthogonal set in the index  $l$  in the interval  $-1 \leq x \leq 1$  (here  $x = \cos\theta$ ). By the same means orthogonality relation for Legendre functions can be written as

$$\int_{-1}^1 P_l(x)P_m(x)dx = \frac{2}{2l+1} \frac{(l+m)!}{(l-m)!} \delta_{lm} \tag{2.1.13}$$

The solution of the laplace equation was decomposed in to a product of factors for the three variables  $r, \theta$  and  $\varphi$ . It is convenient to combine the angular factors and construct orthonormal functions over the unit sphere. The functions  $Q_m(\varphi) = \exp(im\varphi)$  form a complete set of orthogonal functions in the index  $m$  on the interval  $0 \leq \varphi \leq 2\pi$ . The functions  $P_l(\cos\theta)$  form a similar set in the index  $l$  for each  $m$  value in the interval  $-1 \leq \cos\theta \leq 1$ . Therefore their product  $Q_m P_l^m$  [34] will form a complete orthogonal set on the surface of a unit sphere in the two indices  $l, m$ . From the normalization condition it is clear that the normalization function, denoted by  $Y_{lm}(\theta, \varphi)$ , is

$$Y_{lm}(\theta, \varphi) = \sqrt{\frac{2l+1}{4\pi} \frac{(l-m)!}{(l+m)!}} P_l^m(\cos\theta) \exp(im\varphi) \tag{2.1.14}$$

Is spherical harmonics, spherical harmonics for  $l = 1$  dipole,  $l = 2$  quadrupole and  $l = 3$  octupole are given as

$$\begin{aligned}
Y_{10} &= \sqrt{\frac{3}{4\pi}} \cos\theta, & Y_{11} &= -\sqrt{\frac{3}{8\pi}} \sin\theta \exp(i\varphi) \\
Y_{20} &= \frac{1}{2} \sqrt{\frac{5}{4\pi}} (3\cos^2\theta - 1), & Y_{21} &= -\sqrt{\frac{15}{8\pi}} \sin\theta \cos\theta \exp(i\varphi) \\
Y_{30} &= \frac{1}{2} \sqrt{\frac{7}{4\pi}} \sin(5\cos^3\theta - 3\cos\theta) \\
Y_{31} &= -\frac{1}{4} \sqrt{\frac{21}{4\pi}} \sin\theta (5\cos^2\theta - 1) \exp(i\varphi)
\end{aligned} \tag{2.1.15}$$

Now from equation (2.1.11) we get

$$Y_{l,-m}(\theta, \varphi) = (-1)^m Y_{lm}^*(\theta, \varphi) \quad (2.1.16)$$

Which gives a way of generating the unwritten negative m harmonics above. Also, remember, for a given l there are  $2l + 1$  different spherical harmonics:

$$m = l, l - 1, \dots, 0, \dots, -l + 1, -l$$

Also note, that a spherical harmonic, with  $m = 0$  is just the normalisation constant, multiplied by the Legendre polynomial:  $Y_{l0}(\theta, \varphi) = \sqrt{\frac{2l+1}{4\pi}} P_l(\cos\theta)$ . The normalization and orthogonality conditions are:

$$\int_0^{2\pi} d\varphi \int_0^\pi \sin\theta d\theta Y_{l'm'}^*(\theta, \varphi) Y_{lm}(\theta, \varphi) = \delta_{l'l} \delta_{m'm} \quad (2.1.17)$$

the completeness relation, corresponding to  $\sum_{n=1}^{\infty} U_n^*(\eta) U_n(\eta) = \delta(\eta' - \eta)$  is

$$\sum_{l=0}^{\infty} \sum_{m=-l}^l Y_{lm}^*(\theta', \varphi') Y_{lm}(\theta, \varphi) = \delta(\varphi - \varphi') \delta(\cos\theta - \cos\theta') \quad (2.1.18)$$

considering two coordinate vectors  $\vec{x}$  and  $\vec{x}'$ , with spherical coordinates  $(r, \theta, \varphi)$  and  $(r', \theta', \varphi')$  respectively and angle  $\zeta$  between them. From the addition theorem for spherical harmonics we get [43]:

$$P_l(\cos\zeta) = \left( \frac{4\pi}{2l+1} \right) \sum_{m=-l}^l Y_{lm}^*(\theta', \varphi') Y_{lm}(\theta, \varphi) \quad (2.1.19)$$

The expansion for  $\frac{1}{|\vec{r} - \vec{r}'|}$  is

$$\frac{1}{|\vec{r} - \vec{r}'|} = \sum_{l=0}^{\infty} \left( \frac{r'^l}{r^{l+1}} \right) P_l(\cos\zeta) \quad (2.1.20)$$

which is the potential at r due to a unit charge at  $r'$ . By substituting equation (2.1.19) in to (2.1.20) we can find the explicit form

$$\frac{1}{|\vec{r} - \vec{r}'|} = 4\pi \sum_{l=0}^{\infty} \sum_{m=-l}^l \left( \frac{1}{2l+1} \right) \left( \frac{r'^l}{r^{l+1}} \right) Y_{lm}^*(\theta', \varphi') Y_{lm}(\theta, \varphi) \quad (2.1.21)$$

Inserting eqn.(2.1.21) in (2.1.5) we find

$$\vec{A}_\varphi^{(l)} = \hat{e}_\varphi 4\pi \sum_{l=0}^{\infty} \left( \frac{1}{2l+1} \right) \left( \frac{r_{<}^l}{r_{>}^{l+1}} \right) \quad (2.1.22)$$

$$* \sum_{m=-l}^{m=l} Y_{lm}(\theta, \varphi) \int_{r'} \int_{\theta'} \int_{\varphi'} \vec{J}(r')_{\varphi'} Y_{lm}^*(\theta', \phi') r'^2 \sin\theta' dr' d\phi' d\theta'$$

The presence of  $\exp(i\varphi')$  means that only  $m = +1$  will contribute to the sum.

$$\vec{A}_\varphi^{(l)} = \hat{e}_\varphi 4\pi \sum_{l=0}^{\infty} \left( \frac{1}{2l+1} \right) \left( \frac{r_{<}^l}{r_{>}^{l+1}} \right) \quad (2.1.23)$$

$$* Y_{l1}(\theta, \varphi) \int_{r'} \int_{\theta'} \int_{\varphi'} \vec{J}(r')_{\varphi'} Y_{l1}^*(\theta', \varphi') r'^2 \sin\theta' dr' \cos\varphi' d\varphi' d\theta'$$

using eqn. (2.1.4) instead of  $\vec{J}(r')_{\varphi'} = J \cos\varphi'$  follows

$$\vec{A}_\varphi^{(l)} = \hat{e}_\varphi \left( -\frac{|Q|\omega}{4\pi R} \right) 4\pi \sum_{l=0}^{\infty} \left( \frac{1}{2l+1} \right) \left( \frac{r_{<}^l}{r_{>}^{l+1}} \right) \quad (2.1.24)$$

$$* Y_{l1}(\theta, \varphi) \int_{r'} \int_{\theta'} \int_{\varphi'} Y_{l1}^*(\theta', \varphi') r'^2 \sin^2\theta' dr' \cos\varphi' d\varphi' d\theta' \delta(r' - R)$$

Here, we are interested to the exterior point, so  $r_{<} = R, r' \rightarrow R$  and

$r_{>} = r$  refers to the inner and outer region of the neutron star respectively.

$$\text{as } r' \rightarrow R \quad \int dr' r'^2 \delta(r' - R) = R^2$$

$$\vec{A}_\varphi^{(l)} = \hat{e}_\varphi \left( -\frac{|Q|\Omega}{4\pi R} \right) 4\pi R^2 \sum_{l=0}^{\infty} \left( \frac{1}{2l+1} \right) \left( \frac{R^l}{r^{l+1}} \right) \quad (2.1.25)$$

$$* Y_{l1} \int_{\theta'} \int_{\varphi'} Y_{l1}^* \sin^2\theta' \cos\varphi' d\varphi' d\theta'$$

Different poles are derived by assigning different values for  $l$ . We pick

$l = 1, l = 2, l = 3$  for dipole, quadrupole and octupole respectively.

$$\vec{A}_\varphi^{(1)} = \hat{e}_\varphi \left( -\frac{|Q|\Omega}{12\pi R} \right) \left( \frac{4\pi R^3}{r^2} \right) Y_{11} \int_{\theta'} \int_{\varphi'} Y_{11}^* \sin^2\theta' \cos\varphi' d\varphi' d\theta' \quad (2.1.26)$$

Now, inserting the value of  $Y_{11}$  from above we have

$$\vec{A}_\varphi^{(1)} = \hat{e}_\varphi \left( -\frac{|Q|\Omega}{8\pi} \right) \left( \frac{R^2}{r^2} \right) \sin\theta \int_0^\pi \sin^3\theta' d\theta' \int_0^{2\pi} \cos\varphi' \exp(i\varphi') d\varphi' \quad (2.1.27)$$

$$\vec{A}_\varphi^{(1)} = \hat{e}_\varphi \left( -\frac{|Q|\Omega}{3} \right) \left( \frac{R^2}{r^2} \right) \sin\theta \quad (2.1.28)$$

Applying the same method and inserting the value of  $Y_{21}$  from(2.1.15)

$$\vec{A}_\varphi^{(2)} = \hat{e}_\varphi \left( -\frac{|Q|\Omega}{4\pi R} \right) 4\pi R^2 \left( \frac{1}{5} \right) \left( \frac{R^2}{r^3} \right) Y_{21} \int_{\theta'} \int_{\varphi'} Y_{21}^* \sin^2 \theta' \cos \phi' d\varphi' d\theta' \quad (2.1.29)$$

$$\vec{A}_\varphi^{(2)} = \frac{3|Q|\Omega R^3}{4r^3} \sin\theta \cos\theta \quad (2.1.30)$$

$$\vec{A}_\varphi^{(3)} = \hat{e}_\varphi (|Q|\Omega) \left( \frac{R^4}{7r^4} \right) Y_{31} \int_{\theta'} \int_{\varphi'} Y_{31}^* \sin^2 \theta' \cos \phi' d\varphi' d\theta' \quad (2.1.31)$$

Inserting the value of  $Y_{31}$  from(2.1.15)

$$\vec{A}_\varphi^{(3)} = \hat{e}_\varphi (|Q|\Omega) \left( \frac{7R^4}{20r^4} \right) \sin\theta (5\cos^2\theta - 1) \quad (2.1.32)$$

## 2.2 Magnetic Multipolar fields of neutron star

We Consider system of spherical coordinates  $(r, \theta, \varphi)$  where  $r$  is measured from stellar center[36,37],  $\theta$  is the polar angle (in radians) measured from the  $z$  axis and  $\varphi$  is azimuthal angle (in radians) measured from an arbitrary origin .The  $z$ -axis is directed along the dipolar momentum of the star  $\vec{\mu}$ . It is known that magnetic field is the curl of vector potential i.e,

$$\vec{B} = \nabla \times \vec{A} = \frac{1}{r \sin\theta} \begin{pmatrix} \hat{r} & r\hat{\theta} & r\sin\theta\hat{\varphi} \\ \partial_r & \partial_\theta & \partial_\varphi \\ A_r & rA_\theta & r\sin\theta A_\varphi \end{pmatrix}$$

$$\begin{aligned} \vec{B} = & \frac{1}{r \sin\theta} \left[ \frac{\partial}{\partial\theta} (\sin\theta A_\varphi) - \frac{\partial}{\partial\varphi} (A_\theta) \right] \hat{r} \\ & + \frac{1}{r} \left[ \frac{1}{\sin\theta} \frac{\partial}{\partial\varphi} (A_r) - \frac{\partial}{\partial r} (rA_\varphi) \right] \hat{\theta} \\ & + \frac{1}{r} \left[ \frac{\partial}{\partial r} (rA_\theta) - \frac{\partial}{\partial\theta} (A_r) \right] \hat{\varphi} \end{aligned} \quad (2.2.1)$$

In general we can write multipolar fields as

$$\vec{B}^{lm}(r, \theta) = \nabla \times \vec{A}_\varphi^{lm} \quad (2.2.2)$$

In our case  $\vec{A}$  has only an azimuthal component. Therefore, only  $\vec{B}_r^{lm}(r, \theta)$  and  $\vec{B}_\theta^{lm}(r, \theta)$  survive, so that our equation will be

$$\vec{B}_r^{lm}(r, \theta) = \frac{\hat{e}_r}{r \sin \theta} \frac{\partial}{\partial \theta} \left( \vec{A}_\phi^{lm}(r, \theta) \sin \theta \right) \quad (2.2.3)$$

$$\vec{B}_\theta^{lm}(r, \theta) = -\frac{\hat{e}_\theta}{r} \frac{\partial}{\partial r} \left( r \vec{A}_\phi^{lm}(r, \theta) \right) \quad (2.2.4)$$

As usual we use  $l = 1$ ,  $l = 2$  and  $l = 3$  for the dipole, quadrupole and octupole field respectively. If  $m=0$  and  $l$  is arbitrary, then one obtains axially symmetric and uniform multipolar components.

### 2.2.1 Magnetic dipole field of neutron star

Based on the above relation between magnetic field and vector potential we find the dipole field components as shown below

$$B^{(1)}(r, \theta) = \nabla \times \vec{A}_\phi^{(1)} \quad (2.2.5)$$

$$B^{(1)}(r, \theta) = \frac{\hat{e}_r}{r \sin \theta} \left[ \frac{\partial}{\partial \theta} (\sin \theta A_\phi^1) \right] - \frac{\hat{e}_\theta}{r} \left[ \frac{\partial}{\partial r} (r A_\phi^1) \right] \quad (2.2.6)$$

$$= \frac{\hat{e}_r}{r \sin \theta} \frac{|Q|\Omega}{3} \left( \frac{R}{r} \right)^2 \left[ \frac{\partial}{\partial \theta} (\sin^2 \theta) \right] + \frac{\hat{e}_\theta}{r} \frac{|Q|\Omega}{3} \sin \theta R^2 \left[ \frac{\partial}{\partial r} \left( \frac{1}{r} \right) \right] \quad (2.2.7)$$

$$= \frac{\hat{e}_r}{r \sin \theta} \frac{|Q|\Omega}{3} \left( \frac{R}{r} \right)^2 2 \sin \theta \cos \theta - \frac{\hat{e}_\theta}{r} \frac{|Q|\Omega}{3} \sin \theta \left( \frac{R}{r} \right)^2 \quad (2.2.8)$$

$$= \frac{Q\Omega R^2}{3r^3} \cos \theta \hat{e}_r + \frac{Q\Omega R^2}{3r^3} \sin \theta \hat{e}_\theta \quad (2.2.9)$$

The radial and polar components of the dipolar field is written as

$$B_r^{(1)} = \frac{2\mu_d}{3r^3} \cos \theta \hat{e}_r, \text{ and} \quad (2.2.10)$$

$$B_\theta^{(1)} = \frac{\mu_d}{3r^3} \sin \theta \hat{e}_\theta \quad (2.2.11)$$

Where  $\vec{\mu}_d = \mu_d \hat{\mu} = |Q|\Omega R_*^2$  is the dipole moment. A neutron star total magnetic field is given by:  $B_* = B_d + B_q + B_o + \dots$

Hence the dipole moment  $\mu_d$  can be written as

$$\mu_d = B_{*(d)} R_*^3 = |Q|\Omega R_*^2 \quad (2.2.12)$$

In general form magnetic multipole moment is

$$\mu^{lm} = B_*^{lm} R_*^{l+2}$$

## 2.2.2 Magnetic Quadrupolar field of neutron star

Under this topic we consider magnetic fields that are in a "potential state." This terminology, which is common in the solar/stellar physics literature, refers to a magnetic field in which the current density  $\vec{J} = 0$  everywhere within the stellar magnetosphere, and therefore the field  $\vec{B}$  can be written in terms of the gradient of a magnetostatic scalar potential [14,31] so that the intrinsic magnetic field of the star can be written as  $\mathbf{B} = -\nabla\varphi$  [37,19], where the scalar potential of the magnetic field is  $\varphi(r) = \sum ma/|\vec{r} - \vec{r}_a|$ , and  $m_a$  is an analogy of the magnetic charge,  $\vec{r}$  and  $\vec{r}_a$  are the positions of the observer and the magnetic charges respectively. The scalar potential can be represented as a multipole expansion in powers of  $1/r$ . In the near zone limit ( $kr \ll 1$ ), the magnetic field vector  $B^{lm}(r, \theta, \varphi)$ , associated with a given magnetic multipole ( $lm$ ) [38], can be expressed in terms of spherical harmonics  $Y_{lm}(\theta, \varphi)$  (Jackson 1975):

$$B^{lm}(r, \theta, \varphi) = \nabla \left( \frac{Y_{lm}(\theta, \varphi)}{r^{l+1}} \right) \quad (2.2.13)$$

Spherical harmonics are written in terms of the associated Legendre functions as

$$Y_{lm}(\theta, \varphi) = \sqrt{\frac{2l+1}{4\pi} \frac{(l-m)!}{(l+m)!}} P_l^m(\cos\theta) e^{im\varphi}$$

where  $P_l^m(x)$ , is the associated Legendre function, is defined as

$$P_l^m(x) = \frac{(-1)^m}{2^l l!} (1-x^2)^{m/2} \frac{d^{l+m}}{dx^{l+m}} (x^2-1)$$

In a spherical geometry, the components of an individual multipolar magnetic field vectors are written as

$$B_r^{lm}(r, \theta, \varphi) = -4\pi \frac{l+1}{2l+1} \frac{q_{lm}}{r^{l+2}} Y_{lm}(\theta, \varphi) \quad (2.2.14)$$

$$B_\theta^{lm}(r, \theta, \varphi) = \frac{4\pi}{2l+1} \frac{q_{lm}}{r^{l+2}} Y_{lm}^{(1,0)}(\theta, \varphi) \quad (2.2.15)$$

$$B_\varphi^{lm}(r, \theta, \varphi) = \frac{4\pi}{2l+1} \frac{q_{lm}}{r^{l+2}} im \sin\theta Y_{lm}(\theta, \varphi) \quad (2.2.16)$$

where 1 is for m and 0 is for  $\varphi$  in eqn.(2.2.20) i.e polar component.

$$q_{lm} \equiv \int d^3r' r'^l Y_{lm}^*(\theta, \varphi) \rho(\vec{r}') \quad (2.2.17)$$

$$= \int_0^\infty r'^2 dr' \int_0^{2\pi} d\varphi' \int_0^\pi \sin\theta' d\theta' \rho(r', \theta', \varphi') r'^l Y_{lm}^*(\theta', \varphi') \quad (2.2.18)$$

$q_{lm}$  is known as multipole moment of the charge distribution. This moment satisfy the identity  $q_{lm} = (-1)^m q_{l,-m}^*$ . The first few moments are as follows

$$q_{00} = \frac{q}{\sqrt{4\pi}}, \quad q_{10} = \sqrt{\frac{3}{4\pi}} P_z$$

where  $q$  is precisely the total charge of the system and  $P$  is the electric dipole moment. when expressed in terms of spherical polar coordinates,  $x = r \sin\theta \cos\varphi$ ,  $y = r \sin\theta \sin\varphi$  and  $z = r \cos\theta$  using these we have

$$\begin{aligned} q_{11} &= -\sqrt{\frac{3}{8\pi}} \int d^3r' \rho(\vec{r}') r' \sin\theta e^{-i\varphi} = -\sqrt{\frac{3}{8\pi}} \int d^3r' \rho(\vec{r}') (x - iy) = \sqrt{\frac{3}{8\pi}} (p_x - ip_y) \\ q_{20} &= \frac{1}{2} \sqrt{\frac{5}{4\pi}} Q_{33}, \quad q_{21} = -\frac{1}{3} \sqrt{\frac{15}{8\pi}} (Q_{13} - iQ_{23}) \\ q_{22} &= \frac{1}{12} \sqrt{\frac{15}{2\pi}} (Q_{11} - 2iQ_{12} - Q_{22}) \end{aligned} \quad (2.2.19)$$

where,  $Q_{ij}$  is the traceless quadrupole moment tensor, defined by

$$Q_{ij} \equiv \int d^3r' \rho(\vec{r}') (3r'_i r'_j - r'^2 \delta_{ij}) \quad (2.2.20)$$

$i$  and  $j$  stand for cartesian components  $x, y$  and  $z$  or  $1, 2, 3$

$$Tr(Q) = \int d^3r' \rho(\vec{r}') (3r'^2 - 3r'^2) = 0 \quad (2.2.21)$$

Since,  $\sum_i^{1,2,3} r'^2 \delta_{ii} = r'^2 (\delta_{11} + \delta_{22} + \delta_{33}) = 3r'^2$  and  $\sum_i r'_i r'_i = 3r'^2$

The quadrupole moment tensor is symmetric i.e,  $Q_{ij} = Q_{ji}$  this reduces the number of possible independent components to six .As its name suggests it has zero trace so that  $Q_{33} = -Q_{11} - Q_{22}$  [44] and only two of the diagonal components are independent. Thus the tensor can have at most five independent components.

$$Q_{ij} = \begin{pmatrix} Q_{11} & Q_{12} & Q_{13} \\ Q_{21} & Q_{22} & Q_{23} \\ Q_{31} & Q_{32} & Q_{33} \end{pmatrix}$$

If  $m = 0$  and  $l$  is arbitrary, then one obtains axially symmetric and uniform multipolar components [38,40]. The magnetic moment associated with the strength of

the magnetic multipole component ( $lm$ ) at the surface of the star is defined as  $\mu^{lm} = B_s^{lm} R_s^{l+2}$  [33,35,30]. i.e  $\mu^{lm} = B_{*0} R_*^{l+2}$ , where  $B_{*0}$  is the reference magnetic field on the surface of the star and  $R_*$  is the radius of the star. Now applying the above expressions from eqn.(2.2.14 and 2.2.15) we obtain.

$$\begin{aligned}
B_r &= 4\pi \frac{2+1}{4+1} \frac{q_{20}}{r^{l+2}} Y_{20}(\theta, \varphi) & (2.2.22) \\
&= 4\pi \frac{3}{10} \sqrt{\frac{5}{4\pi}} \frac{Q_{33}}{r^4} \sqrt{\frac{5}{4\pi}} \left( \frac{3}{2} \cos^2\theta - \frac{1}{2} \right) \\
&= \frac{3}{2} \frac{Q_{33}}{r^4} \left( \frac{3}{2} \cos^2\theta - \frac{1}{2} \right) \\
\Rightarrow B_r^{(2)} &= \frac{3}{4} \frac{Q_{33}}{r^4} (3\cos^2\theta - 1) = \frac{3}{4} \frac{\mu_q}{r^4} (3\cos^2\theta - 1) & (2.2.23)
\end{aligned}$$

where  $Q_{33} = Q$  is the quadrupole moment and refer to the axis of symmetry as the "direction" of the quadrupole moment ( $\mu_q$ ). If we consider axial multipoles where we have chosen the space-fixed z-axis of the star (the stellar rotation axis) as the symmetry axis of the multipole being considered we can get the known general multipolar magnetic field equation [37,38]. Then spherical field components of an axial multipole ( $B_\varphi = 0$ ) of order  $l$  are given by

$$B_r^l = B_*^{l,pole} \left( \frac{R_*}{r} \right)^{l+2} P_l(\cos\theta) \quad (2.2.24)$$

$$B_\theta^l = \frac{B_*^{l,pole}}{l+1} \left( \frac{R_*}{r} \right)^{l+2} P_{l1}(\cos\theta) \quad (2.2.25)$$

Where  $R_*$  is the star radius,  $r$  is a point external to the star,  $P_{l1}(\cos\theta)$  and  $P_l(\cos\theta)$  are the  $m=1$   $l^{th}$  associated Legendre function and the  $l^{th}$  Legendre polynomial respectively. Now by applying quadrupole field equations we derived above, we calculate the quadrupolar magnetic field components of neutron star. In the same way solving for  $\vec{B}_\theta$  we get

$$B_\theta^{(2)} = \frac{3Q_{33}}{2r^4} \sin\theta \cos\theta = \frac{3\mu_q}{2r^4} \sin\theta \cos\theta \quad (2.2.26)$$

where

$$\mu_q = |Q| \Omega R_*^3 \quad (2.2.27)$$

### 2.2.3 Magnetic Octupolar field

The octupolar field components are also found from previously determined vector potential of  $l = 3$  in chapter one. The result obtained is as follows:

$$B_r^{(3)} \approx \left( \frac{7\Upsilon}{5r^5} \right) \cos\theta(5\cos^2\theta - 3)\hat{e}_r \quad (2.2.28)$$

$$B_\theta^{(3)} \approx \left( \frac{21\Upsilon}{20r^5} \right) \sin\theta(5\cos^2\theta - 1)\hat{e}_\theta \quad (2.2.29)$$

Where  $\Upsilon = \Upsilon\hat{\Upsilon} = |Q|\Omega R_*^4$  is the octupole moment. Following the same fashion the octupole magnetic field components are shown as follows. Hence, from the previous relation

$$\Upsilon = B_{*o} R_*^5 \hat{\Upsilon} \quad (2.2.30)$$

### 2.2.4 Magnetic Dipole-Quadrupole field interaction

Considering that magnetic dipole and quadrupole moments are deflected from the rotation axis by same angle We write magnetic dipole and quadrupole combination (interaction) of neutron star as:

$$B_r^{d+q} = B_r^d + B_r^q = \frac{2\mu_d}{3r^3} \cos\theta \hat{e}_r + \frac{3\mu_q}{4r^4} (3\cos^2\theta - 1)\hat{e}_r \quad (2.2.31)$$

$$B_\theta^{d+q} = B_\theta^d + B_\theta^q = \frac{\mu_d}{3r^3} \sin\theta \hat{e}_\theta + \frac{3\mu_q}{2r^4} \sin\theta \cos\theta \hat{e}_\theta \quad (2.2.32)$$

This interaction become minimum at the point where the first derivative of the equation with respect to  $r$  or  $\theta$  is zero, this happen at:

$$\begin{aligned} -\frac{3\mu_q}{2r\mu_d} &= \frac{\cos\theta}{(3\cos^2\theta - 1)} \quad (\text{for the radial component}) \\ \implies |r| &= \frac{3\mu_q}{2\mu_d \cos\theta} (3\cos^2\theta - 1) \end{aligned} \quad (2.2.33)$$

For instance if we consider  $\theta = 0$  the value of  $r$  at which the interaction is minimum will be  $|r| = \frac{3\mu_q}{\mu_d}$  and so on for other angles. After some calculation for polar component we get

$$-\frac{9\mu_q}{2r\mu_d} = \frac{\cos\theta}{(\cos^2\theta - \sin^2\theta)} \quad (\text{for polar angle } \theta) \quad (2.2.34)$$

$$\implies \cos\theta = \frac{-9\mu_q}{2r\mu_d} (1 - 2\sin^2\theta) \quad (2.2.35)$$

Note,that  $r$  is measured from the center of the star. Here,the field is very

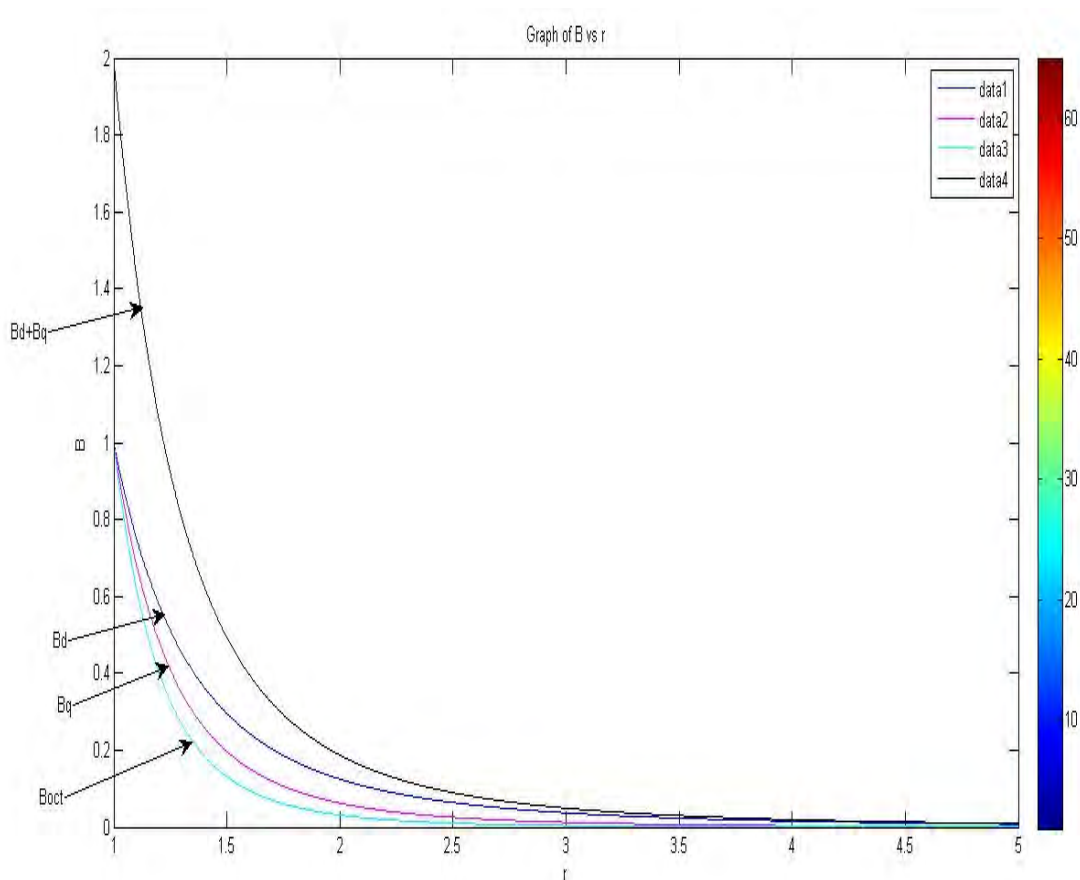


Figure 2.1: Graphical comparison of neutron star magnetic multipole fields and the dipole-quadrupole interaction field vs  $r$ (distance from the center of the star). As seen from the graph octupolar field is fast decaying field as  $r$  increases where as the dipole-quadrupole interaction field is strongest at the surface of the star.

strong for dipole plus quadrupole.Both are reducing at the point far from the star.However,the dipolar field is strongest of all very far from the star because the far field potential is dominated by the first non-zero moment ( $l = 1$ ). According to our assumption on this graph if  $r = 1$  it is on the surface of the star .

# Chapter 3

## Magnetic multipole field line equations of neutron star

Qualitatively, a field line for any vector field  $\vec{V}$  is a curve that is tangential to  $\vec{V}$  at every point along the line. The concept of a field line may be given a mathematical description by writing down the equation for the field line. A convenient starting point is the parametric equations for the field line in cartesian coordinates:

$$\frac{dx}{B_x} = \frac{dy}{B_y} = \frac{dz}{B_z} \quad (3.0.1)$$

The above parametric equations ( may be written in terms of any other orthogonal coordinate system. Accordingly, we will derive magnetic field line equations for different poles and model their geometry.

### 3.1 Magnetic Dipole field line

Here by equation of the field lines We mean an expression of the form  $r = r(\theta)$  which describes the path (shape) of the field lines in a spherical coordinate system. An expression for the field lines of an axisymmetric (axial) multipole of arbitrary degree is derived . In our context the order of a magnetic multipole for ( $l = 1$  and  $l = 2$ ) can be thought of as the number of polarity changes in the surface field between the north and south pole of the star. In this thesis We restrict our attention to axial multipoles, which generate planar field lines. For example, an axial dipole ( $l = 1$ ), quadrupole  $l = 2$ , and octupole ( $l = 3$ ). Throughout our work  $r$  and  $\theta$  are standard spherical polar coordinates, with  $\theta$  measured from the rotation

pole of the star;  $\theta = 0$  corresponds to the stellar rotation pole,  $\theta = \frac{\pi}{2}$  corresponds to the equatorial plane. The origin of the coordinate system is at the center of the star, and thus the stellar surface corresponds to  $r = R_*$ . Only azimuthally symmetric multipoles, known as axial multipoles are considered, i.e.,  $B_\varphi = 0$ . The differential equation describing the path of the field lines in spherical coordinate is

$$dr = dr\hat{r} + rd\theta\hat{\theta} + r\sin\theta d\varphi\hat{\varphi} \quad (3.1.1)$$

In two dimension (2-D) magnetic field can be written as

$$\vec{B} = B_r\hat{r} + B_\theta\hat{\theta} \quad (3.1.2)$$

Here  $l = 1$  dividing these equation one by the other we get

$$\begin{aligned} \frac{B_r^{(1)}\hat{r}}{dr\hat{r}} &= \frac{B_\theta^{(1)}\hat{\theta}}{rd\theta\hat{\theta}} \implies \frac{B_r^{(1)}}{dr} = \frac{B_\theta^{(1)}}{rd\theta} \\ \implies \frac{dr}{r} &= \frac{B_r^{(1)}}{B_\theta^{(1)}}d\theta = K_d \end{aligned} \quad (3.1.3)$$

Where  $k_d$  is a constant related to the field curvature which, upon substituting for  $B_r$  and  $B_\theta$  from above and integrating, yields the well known result .

$$\begin{aligned} \frac{dr}{rd\theta} &= \frac{2\cos\theta}{\sin\theta} \\ \implies \frac{dr}{r} &= 2\cot\theta d\theta \\ \implies \frac{dr}{r} &= \int 2\cot\theta d\theta \\ \implies \ln r &= 2\ln|\sin\theta| + \ln k_d = \ln|\sin\theta|^2 + \ln k_d \\ |r(\theta)| &= k_d \sin^2\theta \end{aligned} \quad (3.1.4)$$

This is the general field line equation for magnetic dipole field. If a particular closed field line loop of the dipole reaches a maximum radial extent of  $r_{max}$  in the stellar equatorial plane, where  $\theta = \pi/2$ . then the integration constant in the above eqn (3.1.4) is equal to  $r_{max}$  [38]. Thus for a dipole the equation of the particular closed field line will be

$$r(\theta) = r_{max}\sin^2\theta \quad (3.1.5)$$

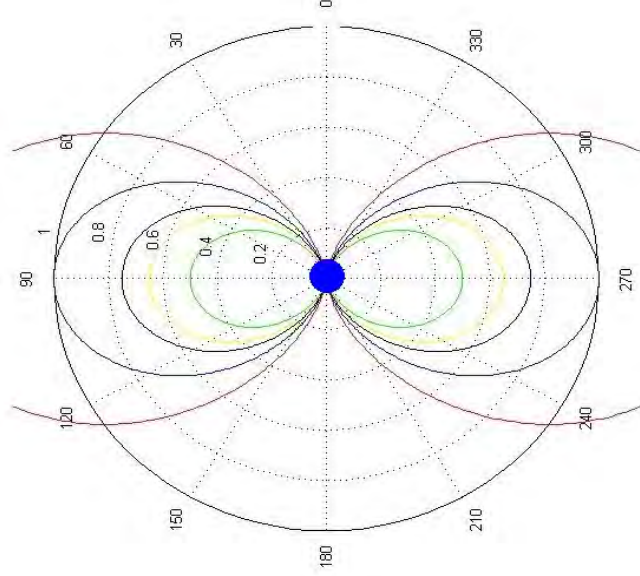


Figure 3.1: Pure magnetic dipole field line geometry for  $K_d > 1$

Different values of  $r_{max}$  correspond to different field lines. there are two lobes in a span of 360 degrees or in the range  $(0, 2\pi)$  for a specific  $k_d$ . where  $k_d$  is a constant related to the dipolar field curvature. For  $r < r_m$  the magnetic energy-density dominates and the field lines are closed. The surfaces where magnetic stress energy balanced with matter stress ( $P + \rho v^2 = \frac{B^2}{8\pi}$ ) i.e, the surface  $\beta = 1$  separates the regions of magnetically dominated and matter dominated plasma ( $\beta = (P + \rho v^2)/\frac{B^2}{8\pi}$ ).

### 3.2 Magnetic Quadrupole field line

Here, again we apply the same method as dipole field line

$$dr = dr\hat{r} + rd\theta\hat{\theta} + r\sin\theta d\varphi\hat{\varphi} \quad (3.2.1)$$

As usual in 2D magnetic field can be written as

$$B = B_r\hat{r} + B_\theta\hat{\theta} \quad (3.2.2)$$

$$\frac{B_r^{(2)}}{dr} = \frac{B_\theta^{(2)}}{rd\theta} \implies \frac{dr}{r} = \frac{B_r^{(2)}}{B_\theta^{(2)}} = k_q \quad (3.2.3)$$

Substituting the quadrupolar field  $B_r^{(2)}$  and  $B_\theta^{(2)}$  from chapter 2 we have

$$\frac{dr}{r} = \frac{\frac{3\mu_q}{4r^4}(3\cos^2\theta - 1)}{\frac{3\mu_q}{2r^4}\sin\theta\cos\theta} \quad (3.2.4)$$

$$\begin{aligned}
&\Rightarrow \int \frac{dr}{r} = \int \frac{1}{2} \frac{(3\cos^2\theta - 1)}{\sin\theta\cos\theta} \\
\ln r &= \frac{1}{2} \int \frac{(3\cos^2\theta - 1)}{\sin\theta\cos\theta} d\theta = \frac{1}{2} \int \frac{3(1 - \sin^2\theta) - 1}{\sin\theta\cos\theta} d\theta \\
&= \frac{1}{2} \int \frac{3 - 3\sin^2\theta - 1}{\sin\theta\cos\theta} d\theta = \frac{1}{2} \int \frac{2 - 3\sin^2\theta}{\sin\theta\cos\theta} d\theta \\
&= \int \frac{1}{\sin\theta\cos\theta} d\theta - \frac{3}{2} \int \frac{\sin^2\theta}{\sin\theta\cos\theta} d\theta \\
&= \int \frac{1}{\sin\theta\cos\theta} d\theta - \frac{3}{2} \int \frac{\sin\theta}{\cos\theta} d\theta \\
&= \int \frac{1}{\sin\theta\cos\theta} d\theta - \frac{3}{2} \int \tan\theta d\theta \\
&= \int \csc\theta \sec\theta d\theta - \frac{3}{2} (-\ln)|\cos\theta| + \ln k_q \\
&= \ln|\tan\theta| + \frac{3}{2} \ln|\cos\theta| + \ln k_q \\
r(\theta) &= \ln|\tan\theta| + \ln|\cos\theta|^{3/2} + \ln k_q \\
|r(\theta)| &= k_q \tan\theta \cos^{3/2}\theta \tag{3.2.5}
\end{aligned}$$

It has four lobes in the range  $(0, 2\pi)$  or in a span of 360 degrees. which have one

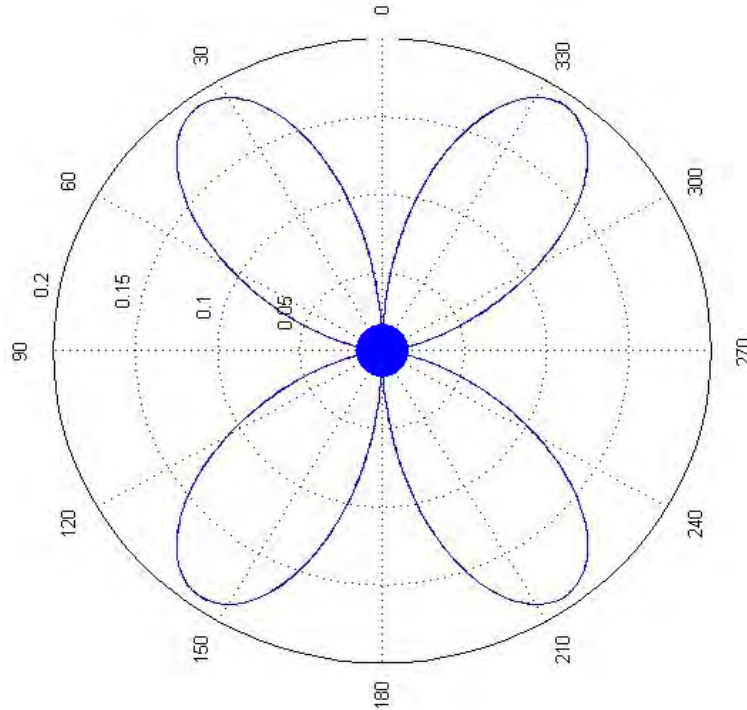


Figure 3.2: Pure quadrupole field line geometry for the solution we derived above.

solution for a single degree in one quadrant for a specific  $k_q$ .

### 3.3 Equadtion of magnetic dipole-quadrupole interaction field line and its geometry

Summing up our previous dipole and quadrupole filed equations as:

$$B_r^{(d+q)} = B_r^{(1)} + B_r^{(2)} \quad , \quad B_\theta^{(d+q)} = B_\theta^{(1)} + B_\theta^{(2)} \quad (3.3.1)$$

Where the indices 1 and 2 indicate the dipole ( $l = 1$ ) and quadrupole ( $l = 2$ ) respectively.

$$B_r^{d+q} = \frac{2\mu_d}{3r^3} \cos\theta + \frac{3Q}{4r^4} (3\cos^2\theta - 1) \quad (3.3.2)$$

$$B_\theta^{d+q} = \frac{\mu_d}{3r^3} \sin\theta + \frac{3Q}{2r^4} \sin\theta \cos\theta \quad (3.3.3)$$

$$\frac{dr}{rd\theta} = \frac{B_r}{B_\theta} \quad (3.3.4)$$

$$\begin{aligned} \implies \int \frac{dr}{r} &= \int \frac{B_r}{B_\theta} d\theta \\ \implies \ln r &= \int \frac{B_r}{B_\theta} d\theta \end{aligned} \quad (3.3.5)$$

Inserting the values of  $B_r$  and  $B_\theta$  from above,we find

$$\begin{aligned} \ln r(\theta) &= \int \frac{\frac{2\mu_d}{3r^3} \cos\theta + \frac{3\mu_q}{4r^4} (3\cos^2\theta - 1)}{\frac{\mu_d}{3r^3} \sin\theta + \frac{3\mu_q}{2r^4} \sin\theta \cos\theta} d\theta \\ &= \int \frac{\frac{2\mu_d}{3r^3} \cos\theta}{\frac{\mu_d}{3r^3} \sin\theta + \frac{3\mu_q}{2r^4} \sin\theta \cos\theta} d\theta + \int \frac{\frac{3\mu_q}{4r^4} (3\cos^2\theta - 1)}{\frac{\mu_d}{3r^3} \sin\theta + \frac{3\mu_q}{2r^4} \sin\theta \cos\theta} d\theta \end{aligned} \quad (3.3.6)$$

the integration yields

$$\begin{aligned} \ln r(\theta) &= \frac{9 \log \sin(\theta/2) / \cos(\theta/2)}{11} - \frac{\log(4 + 18\cos\theta)}{\cos\theta + 1} / 2 \\ &\quad - \frac{162 \log(4 + 18\cos(\theta))}{\cos(\theta) + 1} / (8 - 162) - 3 \log \frac{1/\cos(\theta/2)^2}{2} \\ &\quad + 4 \log \frac{\sin(\theta/2)}{\cos(\theta/2)} / 11 + \ln k \end{aligned} \quad (3.3.7)$$

Simlifying this we arrive at the solution keeping magnetic moments and r constant.

$$|r(\theta)| = k \left[ \frac{(\tan(\theta/2))^{\frac{13}{11}}}{\left[ \left( \frac{4+18\cos\theta}{\cos\theta+1} \right)^{\frac{162}{8-162}-1/2} \left( \frac{1}{1/2\cos\theta+1/2} \right) \right]^{3/2}} \right] \quad (3.3.8)$$

This is the solution we obtained.

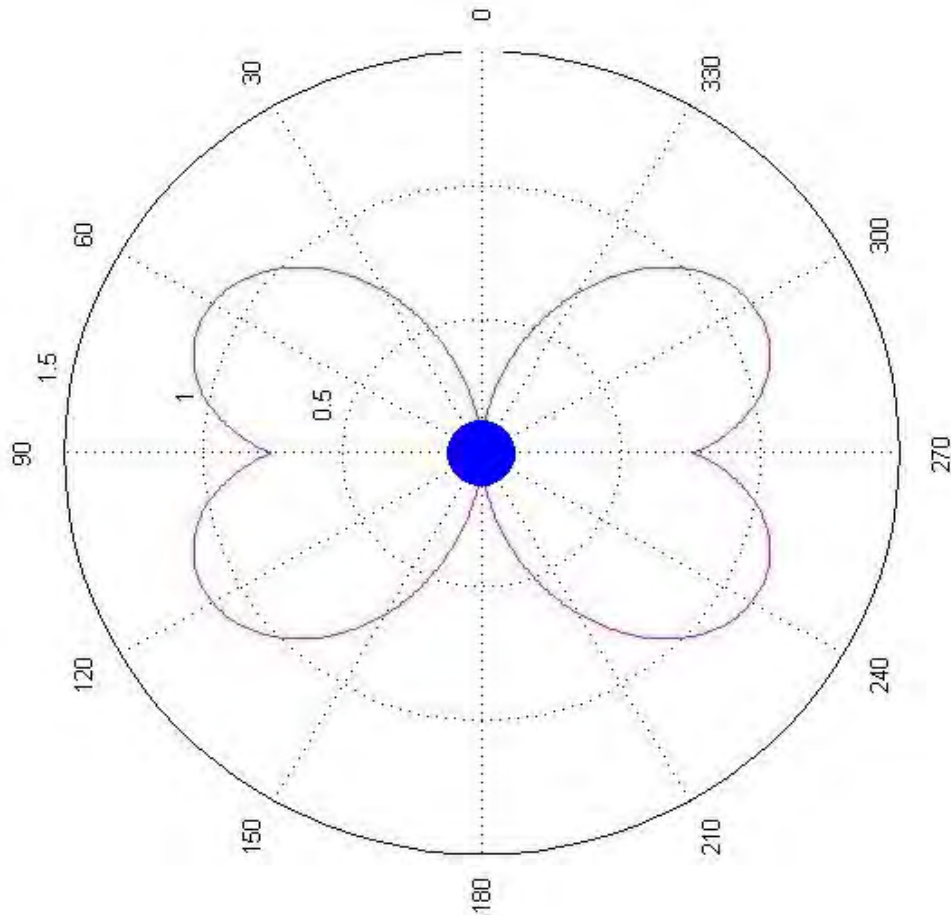


Figure 3.3: Dipole-Quadrupole interaction field line geometry for specific  $k$

Fig.(3.3) and (3.4) are geometries of this field line equation for a single  $k$  and several  $k$ 's respectively. There are two lobes in a span of 360 degrees or in the range  $(0, 2\pi)$  for a specific  $k$ . where  $k$  is a constant related to the interaction field curvature. The geometry is somewhat different in shape from pure dipole field line geometry as it is to be. This field line geometry indicates that there is only one solution for a particular degree in a quadrant. It also shows that the field geometry becomes open at a given distance from the star this means, if we increase the value of  $k$  we can obtain the point at which field lines become open (see fig below).

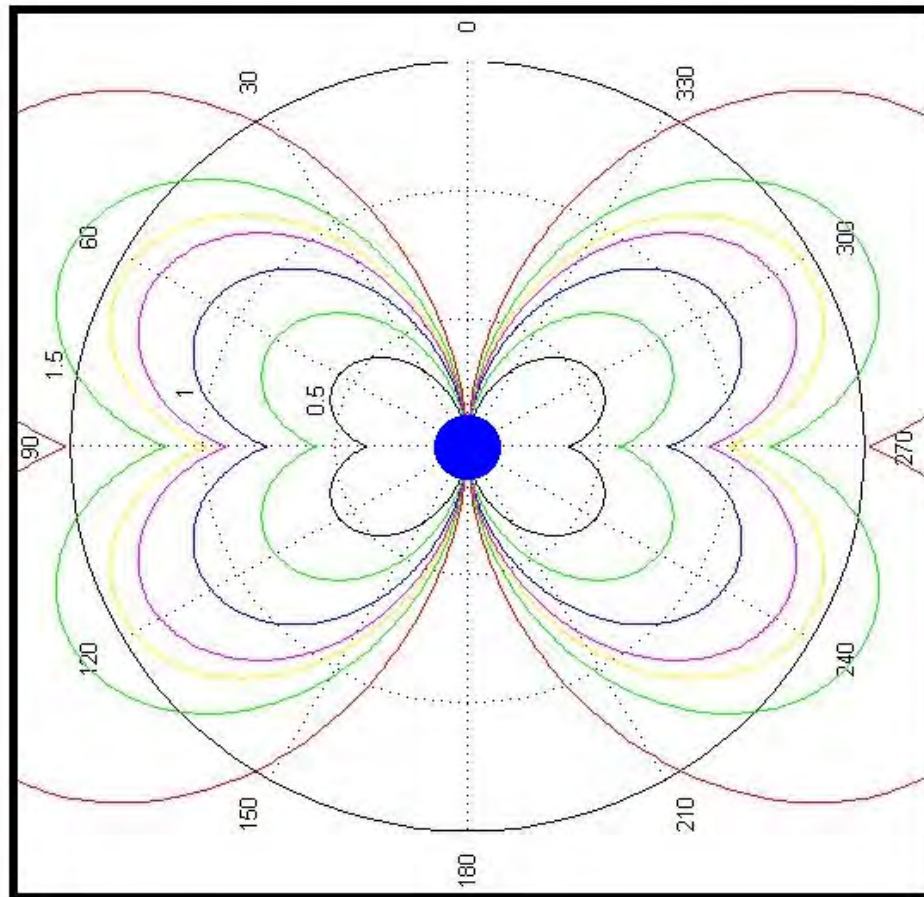


Figure 3.4: Dipole-Quadrupole interaction field lines geometry for  $k = n$ , as number of  $k$  increases large space needed to see full line here.

The geometry for single  $k$  has only one loop in a given quadrant and for many  $k$  there are many loops. Since,  $k$  is related to the interaction field curvature, as the value of this increases the field line opens at a given distance from the surface of the star. This point has some physical meaning or importance to understand the flow of matter to a compact star. The magnetic stresses thus increase much more steeply with decreasing radius than the material stresses do. Therefore, generically one expects that far from the star, material stresses must dominate. Close to the star, magnetic stresses dominate.

# Chapter 4

## Result and Discussion

### 4.1 Result

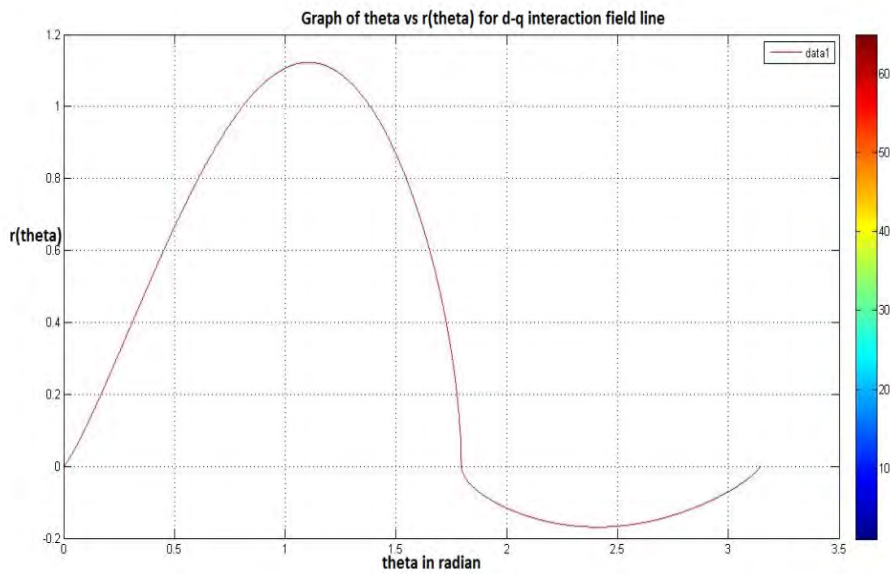


Figure 4.1: Graphical representation of field lines for neutron star magnetic dipole-quadrupole interaction ,where  $\theta$  is in radians.

This is the graph of our field line solution for neutron star dipole-quadrupole magnetic field interaction. It is plotted for the angle of deflection of magnetic moments from axis of rotation versus  $r(\theta)$  between zero degree and  $\pi$  or 3.14 rad and help us to indicate the point of neutral lines. Here the graph indicates there are three neutral lines as we expected. The three neutral lines for this interaction part are the two axes,  $\theta = 0$  and  $\theta = \pi$  and a circle in the plane  $(r, \theta)$  on which  $r$ -solutions correspond to  $\theta$ -angles in the domain  $[\frac{\pi}{2}, \frac{3\pi}{2}]$  radians.

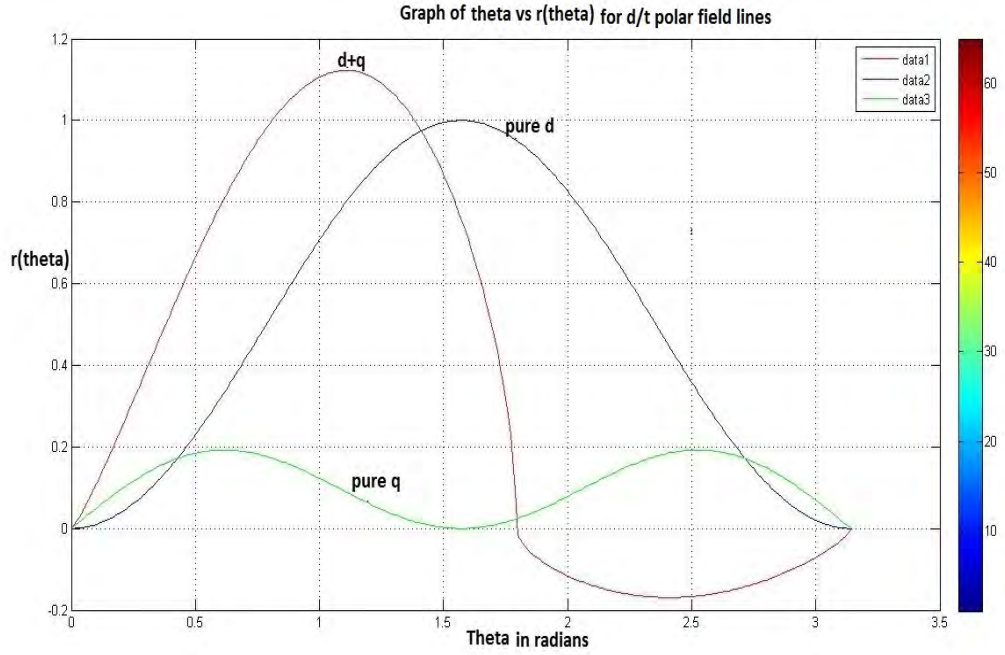


Figure 4.2: Graph of magnetic pure dipole and quadrupole field lines and their interaction.

## 4.2 Discussion

There are three neutral lines for the interaction part as expected :the two axes,  $\theta = 0$  and  $\theta = \pi$  and a circle in the plane  $(r, \theta)$  on which r-solutions correspond to  $\theta$ -angles in the domain  $[\frac{\pi}{2}, \frac{3\pi}{2}]$  degrees.

The three field lines have the same solution at some degrees as both have the same at  $\pi$ . Values of the magnetic field on the lines  $\theta = 0$ , or  $\theta = \pi$  obtained from the equations of magnetic field components, it is clear that on the lines  $\theta = 0$  and  $\theta = \pi$ ,  $B_\varphi(r, \theta) = 0$ , as it is zero every where,  $B_\theta(r, \theta) = 0$ , since  $\sin \theta$  is in factor, but in particular, on the line  $\theta = \pi$ , there is a point at which  $B_r(r, \theta) = 0$ . This point show that it may be a neutral point for particular configurations of the magnetic field in the star magnetosphere. These neutral points may or may not have physical meaning.

# Conclusion

In this paper we have calculated multipolar magnetic fields of neutron star derived from a vector potential produced by spinning surface charges. we investigated magnetic dipole-quadrupole interaction field of neutron star as well as simulated its geometry of field lines in 2D for a single field curvature ( $k = 1$ ) and for different field curvatures ( $k = n$ ). Simulations showed that magnetic field lines are closed if magnetic field is strong enough or (near the surface of the star) and open far from the star this can happen at a maximum radial extent of  $r_{max}$  in the stellar equatorial plane (a given distance from the surface of a star). Geometry of these field lines can affect the size of matter flow to the compact star.

# Appendix

The following constants and expressions have been used in this paper for conversion or direct application.

## A.Constants

- Solar mass ( $M_{\odot}$ ) =  $1.99 \times 10^{33}$  g  $\approx 2 \times 10^{33}$  g
- Solar radius( $R_{\odot}$ ) =  $6.96 \times 10^{10}$  cm  $\approx 7 \times 10^{10}$  cm
- $c = 3 \times 10^8$  m/s is speed of light
- $1T(\text{tesla}) = 10^4G(\text{Gauss})$  are units of magnetic field in mks and cgs systems
- $1\text{parsec}(pc) = 3.08 \times 10^{18}$  cm = 3.26 lightyears.
- 1 second of arc (")= $4.85 \times 10^{-6}$  radians.
- $1AU = 1.50 \times 10^{13}$  cm (the mean distance between the Earth and the Sun).
- $\rho_o \approx 2 \times 10^{14}g/cm^3$  (the central density of atomic nuclei).
- $L_{\odot} = 3.846 \times 10^{33}erg/s$ ,  $\rho_{\odot} = 150g/cm^3$
- Surface gravity of Sun ( $g_{\odot}$ ) =  $2.74 \times 10^4cm/sec^2$
- 1 erg =  $10^{-7}$  Joules
- 1 ev =  $1.602 \times 10^{-19}$  joules
- Mass of electron( $m_e$ )= $9.11 \times 10^{-31}$  kg= $9.11 \times 10^{-28}$  g
- Charge of electron= $1.602 \times 10^{-19}$  c
- Mass of Proton ( $m_p$ ) =  $1.67 \times 10^{-24}$  g
- Mass of neutron ( $m_n$ ) =  $m_p + 2.31 \times 10^{-27}$  g
- h is Planck's constant=  $6.62606957 \times 10^{-34}m^2kg/s$
- Gravitational constant(G)= $6.67 \times 10^{-8}cm^3g^{-1}sec^{-2}$

## B.Abbreviations

- NSs is read as neutron stars

- SGRs is read as soft gamma repeaters
- APXs is read as Anomalous X-ray Pulsars
- GRB is read as Gamma-ray bursts
- MRI(magnetorotational instability)is an instability that arises from the action of the magnetic field in a differentially rotating system (i.e. a disk), and can lead to large scale mixing and turbulence very quickly. (a fluid instability that causes an accretion disk orbiting a massive central object to become turbulent).
- $l = 1,d$  (dipole),  $l = 2 ,q$  (quadrupole) and  $l = 3,oct$ (octupole)

### C.Intermediate mathematical steps

$$\begin{aligned} \ln r(\theta) = & (9 * \mu_q * \log(\sin(\theta/2)/\cos(\theta/2)))/(9 * \mu_q + 2 * \mu_d * r) - \log((4 * \mu_d * r + \\ & 18 * \mu_q * \cos(\theta))/(cos(\theta) + 1))/2 - (3 * \log(1/\cos(\theta/2)^2))/2 + (162 * \mu_q^2 * \log((4 * \\ & \mu_d * r + 18 * \mu_q * \cos(\theta))/(cos(\theta) + 1)))/(162 * \mu_q^2 - 8 * \mu_d^2 * r^2) + (4 * \mu_d * r * \\ & \log(\sin(\theta/2)/\cos(\theta/2)))/(9 * \mu_q + 2 * \mu_d * r) + \ln k \end{aligned}$$

$$\begin{aligned} r(\theta) = & k * \exp((9 * \mu_q * \log(\sin(\theta/2)/\cos(\theta/2)))/(9 * \mu_q + 2 * \mu_d * r) \\ & - \log((4 * \mu_d * r + 18 * \mu_q * \cos(\theta))/(cos(\theta) + 1))/2 \\ & - (3 * \log(1/\cos(\theta/2)^2))/2 + (162 * \mu_q^2 * \log((4 * \mu_d * r + 18 * \mu_q * \cos(\theta))/(cos(\theta) + \\ & 1)))/(162 * \mu_q^2 - 8 * \mu_d^2 * r^2) \\ & + (4 * \mu_d * r * \log(\sin(\theta/2)/\cos(\theta/2)))/(9 * \mu_q + 2 * \mu_d * r)) \end{aligned}$$

$$\begin{aligned} |r(\theta)| = & k(\tan(\theta/2))^{((9*\mu_q+4*\mu_d*r)/(9*\mu_q+2*\mu_d*r)) * } \\ & ((4 * \mu_d * r + 18 * \mu_q * \cos(\theta))/(cos(\theta) + 1))^{((162*\mu_q^2)/(162*\mu_q^2-8*d^2*r^2)-1/2)} / \\ & (1/(cos(\theta)/2 + 1/2))^{(3/2)} \end{aligned}$$

$$\begin{aligned} \int_{all} Y_{lm}(\theta, \varphi) Y_{l'm'}^*(\theta', \varphi') d\Omega = & \delta_{mm'} \delta_{ll'}, \quad d\Omega = \sin\theta d\theta d\varphi \\ \int_0^{2\pi} e^{-im\varphi} d\varphi = & 2\pi \delta_{m0} \\ \int_0^{2\pi} \int_0^\pi Y_{lm}(\theta, \varphi) Y_{l'm'}^*(\theta', \varphi') \sin\theta d\theta d\varphi = & \int_0^{2\pi} \int_{-1}^1 Y_{lm}(\theta, \varphi) Y_{l'm'}^*(\theta', \varphi') d(\cos\theta) d\varphi \\ = & \delta_{mm'} \delta_{ll'} \end{aligned}$$

# References

- [1] G. S. Bisnovaty-Kogan, Stellar physics: Stellar Evolution and Stability, (Springer-Verlag,Berlin, 2002),Vol. 2.
- [2] M. A. Seeds, Horizons: Exploring the Universe, (Wadsworth, 1995).
- [3] V. A. Urpin, S. A. Levshakov and D. G. Yakovlev, Mon. Not. astr. Soc. **219**, 703 - 717 (1986).
- [4] M. Camenzind, Compact Objects in Astrophysics, (Springer-Verlag, Berlin, 2007).
- [5] J. M. Cordes, R.W. Romani and Lundgren,Nature S. C.133-362 (1993)
- [6] P. Riley, J. A. Linker, Z. Miki , R. Lionello, S. A. Ledvina, and J. G. Luhmann, A comparison between global solar magnetohydrodynamic and potential field source surface model results,Astrophys.J.**653**,1510-1516 (2006).
- [7] C. Giunti, W.K. Chung , Fundamentals of Neutrino Physics and Astrophysics, (Oxford University Press ,2007)
- [8] A. Ehreiser, On the evolution of compact objects and plasma physics in weak and strong gravitational and electromagnetic fields, (Max Planck Institute for Radio astronomy, Bonn,2010).
- [9] F.Zwicky and W. Baade,1934c,"Supernovae and Cosmic rays," Phys.Rev.**45**,138.
- [10] K. Ioka and M. Sasaki, The Astrophysical Journal,**600**:296-316 (2004).
- [11] F. C. Michael, Theory of Neutron Star Magnetospheres (Chicago University Press,1991).
- [12] Dr. rer. nat.,Magnetized Neutron Star, (Tubingen,2010)
- [13] J.-L.Tassoul,Stellar Rotation (Cambridge University Press,Cambridge,2000).

- [14] S. Weinberg, Gravitation and Cosmology: Principles and Applications of The General Theory of Relativity, ( John Wiley and Sons, 1972).
- [15] A. Whitehead, The Physics of Neutron Stars, Physics **518**, (2009).
- [16] M. Van der Klis and A. Alpar, The Many Faces of Neutron Stars (1997).
- [17] J.-F. Donati and J. D. Landstreet, Magnetic fields of non-degenerate stars, Annu. Rev. Astron. Astrophys. **47**, 333-370 (2009).
- [18] D. Prialnik, An introduction to the Theory of Stellar Structure and Evolution, Cambridge University Press (2000).
- [19] J. Chadwick, Possible existence of a neutron, Nature 129-312 (1932).
- [20] R. C. Duncan , C. Thompson and C. Kouveliotou, Magnetars, (Scientific American, 2003).
- [21] I. Bombaci and B. Datta, Astrophysics. J. **520**, L69(200); [arXiv:astro-ph/0001478].
- [22] R. Heras, Electromagnetic Radiation from Pulsars and Magnetars, Ed. Wojciech (2012)
- [23] E. N. Parker, Dynamics of the interplanetary gas and magnetic fields, Astrophys. J. **128**, 664-677 (1958)
- [24] K. H. Schatten, J. M. Wilcox, and N. F. Ness, A model of interplanetary and coronal magnetic fields, Sol. Phys. **6**, 44
- [25] C.R. Kitchin, Stars: Nebulae and the Interstellar Medium (Adam Hilger, 1987).
- [26] H. C. Spruit, Cosmic Magnetic Fields: From Planets, to Stars and Galaxies. Eds. K (2008)
- [27] C. G. Gray, G. Karl, and V. A. Novikov, Quadrupolar contact fields: Theory and applications, Am. J. Phys. **77**, 807-817 (2009).
- [28] B. Thide, Electromagnetic field theory, (Uppsala University press, Sweden, 2000).
- [29] N. Ivanova and R. E. Taam, Magnetic braking revisited, Astrophys. J. **599**, 516-521 (2003).
- [30] S. G. Gregory, M. Jardine, C. G. Gray, and J.-F. Donati, The magnetic fields of forming solar-like stars, Rep. Prog. Phys. **73**, 126-901 (2010).
- [31] J. D. Jackson, Classical Electrodynamics, 3rd ed. (John Wiley, 1999).
- [32] D. J. Griffiths , Introduction to electrodynamics, 3rd ed. (Upper Saddle

- River, New jersey, 1999)
- [33] C. Cameron, T. J. Harries, S .V . Jeffers, and F . Paletou, Magnetic fields and accretion flows on the classical T Tauri star V2129 Oph, Mon. Not. R.Astron.Soc.**380**,12971312 (2007).
  - [34] H. W . Wyld, Mathematical Methods for Physics, 2nd ed. (Benjamin/Cummings, Reading MA, 1999).
  - [35] S .G . Gregory, S. P. Matt, J. F. Donati, and M. ardine, The non-dipolar magnetic fields of accreting T Tauri stars,Mon.R.Astron. Soc.**389**,1839-1850 (2008).
  - [36] J. Frank , A. King and D. Raine, Accretion power in astro physics, 3rd ed. (Cambridge University Press, 2002)
  - [37] B. Jeffreys, Derivations of the equation for the field lines of an axisymmetric multipole, Geophys. J. **92**, 355-356 (1988).
  - [38] D. M. Willis and L. R. Young, Equation for the field lines of an axisymmetric magnetic multipole, Geophys. J. R. Astr. Soc. **89**, 1011-1022 (1987).
  - [39] P. Ghosh,Rotation and accretion powered pulsars,(World Scientific Series in Astronomy and Astrophysics,2007), Vol. 10.
  - [40] L. Kirkup, Magnetic field line simulation using a microcomputer, Phys. Educ. **21**, 107-110 (1986).
  - [41] M. van Hoven and Y. Levin. Magnetar Oscillations I: strongly coupled dynamics of the crust and the core. (ArXiv e-prints 1006.0348V, 2010).
  - [42] E. Kreyszig, Advanced Engineering Mathematics, 8th ed. (John Wiley and Sons, New York, 1999).
  - [43] C. G. Gray, Magnetic multipole expansions using the scalar potential, Am. J. Phys. **47**,457-459 (1979).
  - [44] C. Vaz, Electrodynamics, 1st ed. (University of Cincinnati,2006)

## DECLARATION

I hereby declare that this thesis is my original work, has not been presented for a degree in any other university and that all the sources of material used for the thesis have been dully acknowledged.

Name: Gemechu muleta Kumssa

Signature:.....

This thesis has been submitted for examination with my approval as university advisor.

Name: Dr.Legesse Wetro

Signature:.....

Place and time of submission:

Depatement of Physics

Addis Ababa University

June 2013